AD-A126 202 THEORY OF REACTIONS AT A SOLID SURFACE(U) ROCHESTER UNIV NY DEPT OF CHEMISTRY T F GEORGE ET AL. MAR 83 UROCHESTER/DC/83/TR-30 N00014-80-C-0472 1/1

UNCLASSIFIED F/G 20/5 NL

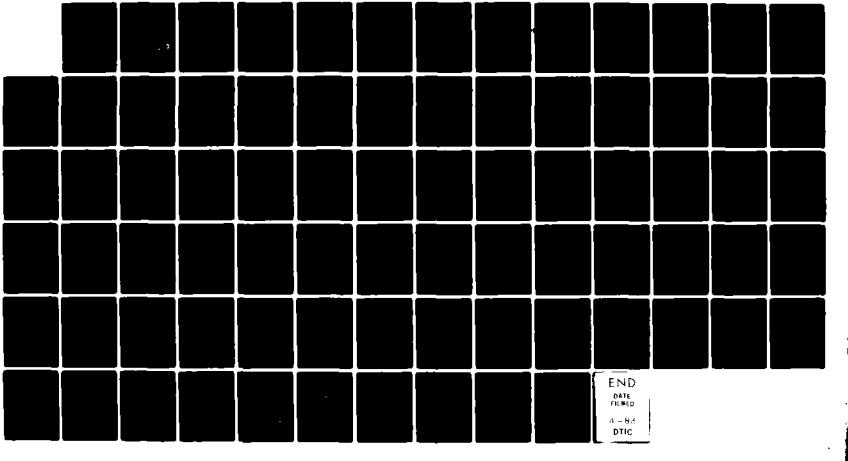

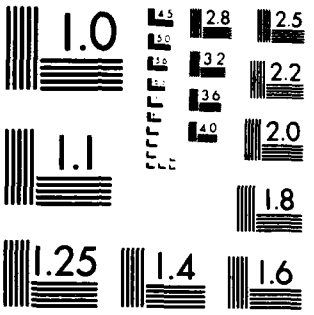

(5)

OFFICE OF NAVAL RESEARCH

Contract N00014-80-C-0472

Task No. NR 056-749

TECHNICAL REPORT No. 30

Theory of Reactions at a Solid Surface

by

Thomas F. George, Ki-Tung Lee, William C. Murphy,
Michael Hutchinson and Hai-Woong Lee

Prepared for Publication

in

The Theory of Chemical Reaction Dynamics
edited by Michael Baer
CRC Press, Baco Raton, Florida

University of Rochester
Department of Chemistry
Rochester, New York 14627

March 1983

Unclassified

SECURITY CLASSIFICATION OF THIS PAGE (When Data Entered)

REPORT DOCUMENTATION PAGE		READ INSTRUCTIONS BEFORE COMPLETING FORM
1. REPORT NUMBER UROCHESTER/DC/83/TR-30	2. GOVT ACCESSION NO. AD-A126 [illegible]	3. RECIPIENT'S CATALOG NUMBER
4. TITLE (and Subtitle) Theory of Reactions at a Solid Surface		5. TYPE OF REPORT & PERIOD COVERED
		6. PERFORMING ORG. REPORT NUMBER
7. AUTHOR(s) Thomas F. George, Ki-Tung Lee, William C. Murphy, Michael Hutchinson and Hai-Woong Lee		8. CONTRACT OR GRANT NUMBER(s) N00014-80-C-0472
9. PERFORMING ORGANIZATION NAME AND ADDRESS Department of Chemistry University of Rochester Rochester, New York 14627		10. PROGRAM ELEMENT, PROJECT, TASK AREA & WORK UNIT NUMBERS NR 056-749
11. CONTROLLING OFFICE NAME AND ADDRESS Office of Naval Research Chemistry Program Code 472 Arlington, Virginia 22217		12. REPORT DATE March 1983
		13. NUMBER OF PAGES 73
14. MONITORING AGENCY NAME & ADDRESS(if different from Controlling Office)		15. SECURITY CLASS. (of this report) Unclassified
		15a. DECLASSIFICATION/DOWNGRADING SCHEDULE

16. DISTRIBUTION STATEMENT (of this Report)

This document has been approved for public release and sale; its distribution is unlimited.

17. DISTRIBUTION STATEMENT (of the abstract entered in Block 20, if different from Report)

18. SUPPLEMENTARY NOTES

Prepared for publication in The Theory of Chemical Reactions, edited by Michael Baer, CRC Press, Baco Raton, Florida.

19. KEY WORDS (Continue on reverse side if necessary and identify by block number)

REACTIONS AT SURFACES
BOND BREAKING AND FORMATION
ATOM/MOLECULE-SURFACE SCATTERING
RECOMBINATION
ADSORPTION
DESORPTION
LASER-STIMULATED PROCESSES
CLASSICAL THEORY
QUANTUM MECHANICAL THEORY

20. ABSTRACT (Continue on reverse side if necessary and identify by block number)

Theories and computational procedures are reviewed for processes involving bond breaking and formation at a solid surface. These processes include reactive scattering, recombination, adsorption and desorption. The article ends with a discussion of theoretical techniques for describing how some of the above processes are induced or modified by laser radiation.

DD FORM 1 JAN 73 1473 EDITION OF 1 NOV 65 IS OBSOLETE
S/N 0102-LF-014-6601

Unclassified

SECURITY CLASSIFICATION OF THIS PAGE (When Data Entered)

to appear as a chapter in
The Theory of Chemical Reaction Dynamics
edited by Michael Baer
CRC, Baco Raton, Florida

THEORY OF REACTIONS AT A SOLID SURFACE

Thomas F. George, Ki-Tung Lee, William C. Murphy and Michael Hutchinson
Department of Chemistry, University of Rochester
Rochester, New York 14627

and

Hai-Woong Lee
Department of Physics, Oakland University
Rochester, Michigan 48063

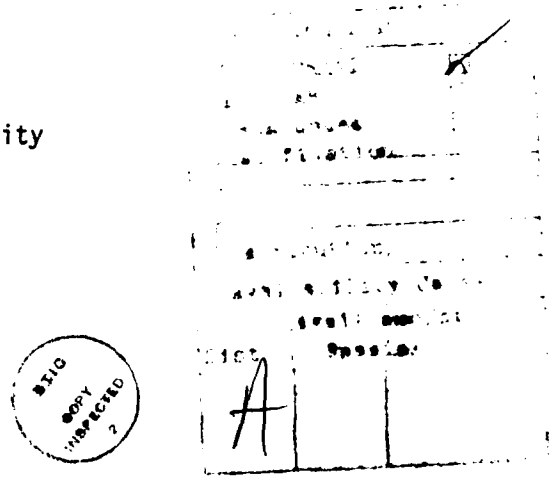

Abstract

Theories and computational procedures are reviewed for processes involving bond breaking and formation at a solid surface. These processes include reactive scattering, recombination, adsorption and desorption. The article ends with a discussion of theoretical techniques for describing how some of the above processes are induced or modified by laser radiation.

CONTENTS

I. INTRODUCTION

Among the chemical reactions of interest to the chemical industry and community in general, the number occurring at a gas-solid interface is far greater than that in the pure gas phase. However, the most thorough analyses of reaction dynamics at the microscopic level have been performed for gas-phase processes, both experimentally and theoretically. In regard to experiments on gas-surface reactions, there are special difficulties such as preparing a clean, specific crystal face which are not present in gas-phase situations. The theoretical problems arise from the many-body aspect of surface processes, where one must deal with the motions of many more nuclei than say, for a three-body rearrangement gas-phase reaction. Nevertheless, strong progress during the past five to ten years has been made in the laboratory and on the development of appropriate theories for understanding the detailed, microscopic dynamics of reactions at a gas-surface interface. Aside from representing a major area of basic research in chemical kinetics and physical chemistry, such studies are leading to an understanding of practical chemical processes such as associated with heterogeneous catalysis.

In this review article we shall address some key advances in the theory of reactions at a gas-solid interface. We shall regard the term "reaction" in a broad sense to apply to any process involving bond breaking and/or bond formation. We shall direct our attention to four general types of processes: reactive scattering, recombination, adsorption and desorption. The first of these is discussed in Sec. II. Two different types of reactions are considered: (1) a gaseous molecular

ion reacts with surface atoms via several steps, and (2) a gaseous atom undergoes a direct reactive encounter with an adspecies. Both quantum mechanical and classical models are utilized, where the latter involves the intergration of classical trajectories leading to the solution of the Generalized Langevin Equation. The second process (Sec. III) is actually a combination of the other three, since it involves adsorption of a gaseous molecule to result in atomic adspecies and then recombination and desorption to form to a gaseous molecule again. Similar techniques, based on potential energy hypersurfaces for the collision dynamics, are used to describe these first two processes.

The third process is discussed in Sec. IV, and here the role of excited electronic states and the coupling of nuclear and electronic degrees of freedom are included in a description of the adsorption event. The fourth process where an adsorbed species leaves the surface is considered in terms of single-phonon and also multiphonon transitions within the solid.

Finally, recent theoretical advances in describing how laser radiation induces or modifies surface rate processes are reviewed. Models for laser-induced desorption are presented, and some ideas on how the excitation of surface states in semiconductors and metals affects charge exchange processes such as ion neutralization are discussed.

II. REACTIVE SCATTERING

A. Formation of Binary Compounds $M_\alpha X_\beta$: Bombarding Clean Surfaces of Pure Metal M with Beams of Diatomic Homonuclear Cations X_2^+

A simple quantum mechanical model[1] has been developed to study a special class of gas-surface reactions, namely

$$\alpha M(s) + \frac{\beta}{2} X_2^+(g) \rightarrow M_\alpha X_\beta(s), \tag{1}$$

where X_2^+ is a diatomic homonuclear cation and M a metal. The overall reaction is modelled by a four-step process

$$X_2^+(g) + e^-(s) \rightarrow X_2(g) \tag{2}$$

$$X_2(g) \rightarrow 2X(g) \tag{3}$$

$$X(g) \rightarrow X(s) \tag{4}$$

$$\alpha M(s) + \beta X(s) \rightarrow M_\alpha X_\beta(s), \tag{5}$$

where g and s denote the gaseous and solid phases, respectively. The development of the model is based on the physical interpretation of experimental observations. The first step describes the incoming cations neutralized via various possible electron transfer processes. The second step represents impact dissociation of X_2 molecules. The third step describes the penetration of the nascent X atom into the metal, its de-excitation and thermalization. Finally, the bond of interest is formed.

1. Neutralization of X_2^+

The neutralization process is treated by a simplified quantum mechanical procedure involving resonance (RN) and Auger (AN) processes:[2]

$$\text{(RN)}\ X_2^+(\mu^+, \nu^+, J^+) + e^-(s, \epsilon, k_1) \rightarrow X_2(\mu, \nu, J) \tag{6}$$

$$(AN)\ X_2^+(\mu^+, \nu^+, J^+) + e^-(s, \varepsilon, k_1) + e^-(s, \varepsilon_2 k_2) \rightarrow X_2(\mu, \nu, J) + e^-(c, \varepsilon_3 k_3) \tag{7}$$

Here, $e^-(s, \varepsilon_i k_i)$ $i = 1, 2$ denotes an electron in the metallic valence band with energy ε_i and momentum k_i and $e^-(c, \varepsilon_3 k_3)$ denotes an electron in the conduction band or vacuum continuum of states characterized by energy ε_3 and momentum k_3. (μ^+, ν^+, J^+) and (μ, ν, J) are the electronic, vibrational and rotational states of the cations and molecules, respectively. The transition rates for these processes are estimated by the Fermi golden rule.[3] With the assumptions that only the electronic component of the cation-metal long-range interaction is critical for these rates, that the electronic, vibrational and rotational motions of X_2^+ and X_2 are separable even at small distances away from the surface, and that the lattice vibrations do not participate in the neutralization processes, the transition rate is given by

$$A_r[i \rightarrow f;\ \ell(t)] = \frac{2\pi}{\hbar}|\langle \mu^+, \varepsilon_1 k_1|\hat{O}_r(\ell)|\mu\rangle|^2 |\langle \mu^+, \nu^+ J^+|\mu, \nu J\rangle|^2 \delta[E(\mu^+\nu^+J^+) - E(\mu\nu J), \varepsilon_1] \tag{8}$$

$$A_a[i \rightarrow f;\ \ell(t)] = \frac{2\pi}{\hbar}\ |\langle \mu^+, \varepsilon_1 k_1, \varepsilon_2 k_2|\hat{O}_a(\ell)|\mu, \varepsilon_3 k_3\rangle|^2 |\langle \mu^+\nu^+J^+|\mu\nu J\rangle|^2 \delta[E(\mu^+\nu^+J^+) - E(\mu\nu J), \varepsilon_1 + \varepsilon_2 - \varepsilon_3] \tag{9}$$

Here, $\hat{O}_{r,a}(\ell)$ denotes the electronic interaction operators responsible for the resonance neutralization and Auger neutralization, respectively. $\ell = \ell(t)$ is the distance between the cation and the surface, $E(\mu^+\nu^+J^+)$ and $E(\mu\nu J)$ are the energies of the cationic and molecular rovibronic states, and δ is a delta function. According to the assumption of

separability, the square modulus of the overlap integral $\langle \mu^+\nu^+J^+|\mu\nu J\rangle$ is given by Franck Condon factor $S(\mu^+\nu^+, \mu\nu)$ and Hönl-London factor $F(\mu^+\nu^+J^+, \mu\nu J)$:[4]

$$|\langle \mu^+\nu^+J|\mu\nu J\rangle|^2 = S(\mu^+\nu^+, \mu\nu)\, F(\mu^+\nu^+J^+, \mu\nu J). \tag{10}$$

Integrating the transition rate with time yields the transition probability, $P_z(i \to f)$, $z = r,a$. The probabilities $P_z(\mu^+\nu^+J^+ \to \mu\nu J)$ are the sums of the transition probabilities $P_z(i \to f)$, with the summation being extended over all metal states whose energies are comparable with the energy conservation

$$\varepsilon_1 = E(\mu^+\nu^+J^+) - E(\mu\nu J) \qquad \text{for RN} \tag{11}$$

$$\varepsilon_1 + \varepsilon_2 - \varepsilon_3 = E(\mu^+\nu^+J^+) - E(\mu\nu J) \qquad \text{for AN} \tag{12}$$

Combining Eqs. (8) - (12), the probabilities $P_z(\mu^+\nu^+J^+ \to \mu\nu J)$ can be written as

$$P_r(\mu^+\nu^+J^+, \mu\nu J) = \frac{2\pi}{\hbar} S(\mu^+\nu^+, \mu\nu)\, F(\mu^+\nu^+J^+, \mu\nu J)$$

$$\int_{t_0}^{t_f} dt \int_{\varepsilon_b}^{\varepsilon_f} d\varepsilon_1 \int d\hat{k}_1 |\langle \mu^+, \varepsilon_1 k_1|\hat{O}_r(\ell)|\mu\rangle|^2$$

$$\delta[E(\mu^+\nu^+J^+) - E(\mu, \nu J), \varepsilon_1], \tag{13}$$

$$P_a(\mu^+\nu^+J^+, \mu\nu J) = \frac{2\pi}{\hbar} S(\mu^+\nu^+, \mu\nu)\, F(\mu^+\nu^+J^+, \mu\nu J)$$

$$\int_{\varepsilon_b}^{\varepsilon_f} d\varepsilon_1 \int_{\varepsilon_b}^{\varepsilon_f} d\varepsilon_2 \int_{\varepsilon_f}^{\infty} d\varepsilon_3 \int_{(\varepsilon_1)} d\hat{k}_1 \int_{(\varepsilon_2)} d\hat{k}_2 \int_{(\varepsilon_3)} d\hat{k}_3$$

$$\int_{t_0}^{t_f} dt |\langle \mu^+, \varepsilon_1 k_1 \varepsilon_2 k_2|\hat{O}_a(\ell(t))|\mu, \varepsilon_3 k_3\rangle|^2$$

$$\times \delta[E(\mu^+, \nu^+, J^+) - E(\mu\nu J), \varepsilon_1 + \varepsilon_2 - \varepsilon_3]. \tag{14}$$

In Eqs. (13) and (14), the highest and lowest energies of the metal valence band are denoted by ε_f and ε_b, and $\int_{(\varepsilon_i)} d\hat{k}_i$ denotes the integration over all the possible directions of the momentum k_i associated with the energy level ε_i. All the dynamic information is contained in the function $\ell(t)$. Both processes are assumed to occur within the range $\ell(t_0) - \ell(t_f)$. Under the experimental condition that the incoming kinetic energy is small, ≤ 30 eV, and that the time of flight thro the region of long-range interaction is long enough whereby the com ed neutralization (RN + AN) is nearly 100% efficient, a knowledge of ℓ is unnecessary, and the integration over time can be performed by the mean-value theorem, namely,

$$\int_{t_0}^{t_f} dt\, A_{r,a}^{\text{electronic}}(\ell(t)) = A_{r,a}^{\text{electronic}}(\bar{\ell}) \times |t_0 - t_f|, \tag{15}$$

where $\ell(t_f) \leq \bar{\ell} \leq \ell(t_0)$, and $A_{r,a}^{\text{electronic}}$ are electronic components of the transition rate. Finally, $A_{r,a}^{\text{electronic}}(\bar{\ell})$ are replaced by their "state averages", denoted by $\bar{A}_{r,a}$. Introduction of these approximations into Eqs. (13) and (14) yields the following expression for $P_{r,a}(\mu^+\nu^+J^+ \rightarrow \mu\nu J)$:

$$P_{r,a}(\mu^+\nu^+J^+ \rightarrow \mu\nu J) = \frac{2\pi}{\hbar} |t_0 - t_f| \bar{A}_{r,a} N(\mu^+) N(\mu) \times \tilde{\rho}_{r,a}(T)$$

$$S(\mu^+\nu^+, \mu\nu)\, F(\mu^+\nu^+J^+, \mu\nu J). \tag{16}$$

Here, $N(\mu^+)$ and $N(\mu)$ are the multiplicities of the μ^+-th cationic and μ-th moleuclar states, and T equals $E(\mu\nu J) - E(\mu^+\nu^+J^+)$. The function

$\tilde{\rho}_{r,a}(T)$ is defined as follows:

$$\tilde{\rho}_r(T) = \rho_s(T) \tag{17}$$

$$\tilde{\rho}_a(T) = \int_{\varepsilon_1(T)}^{\varepsilon_f} d\varepsilon_1 \int_{\varepsilon_2(T,\varepsilon_1)}^{\varepsilon_f} d\varepsilon_2 \int_{\varepsilon_f}^{2\varepsilon_f - T} d\varepsilon_3 \, \rho_s(\varepsilon_1)\rho_s(\varepsilon_2)\rho_c(\varepsilon_3), \tag{18}$$

where $\rho_s(\varepsilon)$ is the density of electronic states in the metallic valence band and $\rho_c(\varepsilon)$ is the density of states in the conduction band and vacuum continuum. The integration limit is defined as the following: the minimum energy for an electron either in the conduction band or in the vacuum continuum is the Fermi energy ε_f, and the maximum energy is given by Eq. (12),

$$\varepsilon_3^{max} = \varepsilon_1(=\varepsilon_f) + \varepsilon_2(=\varepsilon_f) - T. \tag{19}$$

Similarly, the limits for the ε_2 and ε_1 integrals are given by

$$\varepsilon_2(T, \varepsilon_1) = \max(\varepsilon_f + T - \varepsilon_1, \varepsilon_b) < \varepsilon_2 < \varepsilon_f \tag{20}$$

and

$$\varepsilon_1(T) = \max(T, \varepsilon_b) < \varepsilon_1 < \varepsilon_f, \tag{21}$$

respectively, Information about $\rho_s(\varepsilon)$ and $\rho_c(\varepsilon)$ can usually be obtained experimentally from Auger electron spectroscopy[4] or theoretically such as from the free-electron model.[5] The neutralization probabilities are then calculable quantities, provided the "state-averaged" matrix elements $\bar{A}_{r,a}$ are known.

2. Phenomenological Treatment

The probability of X_2 dissociation is assumed to depend on the kinetic energy E_k and the dissociation energy $D = D(\mu\nu J)$, but insensitive to other specifics of the $(\mu\nu J)$ state. A statistical model of Kassel[6] can be applied to the dissociation probability,

$$P(E_k, D) = 0 \qquad \text{for } E_k \leq D \tag{22}$$

$$P(E_k, D) = 1 - \left(\frac{D}{E_k}\right)^{p-1} \qquad \text{for } E_k \geq D, \tag{23}$$

in which p is the number of normal vibrational modes of the complex. This model is justified if the diatom forms some kind of complex with the metal. Let $R(X_2^+, E_k)$ denote the dose of X_2^+ cations in the molecular beam at the kinetic energy E_k and $W(\mu^+, \nu^+, J^+)$ present in the beam at the distance $\ell(t_0)$ from the surface. Then $R(X, E_k)$, the dose of atoms X received by the metal surface is given by

$$R(X, E_k) = 2P_t \int_0^\infty dD\ P(E_k, D)\ R(X_2, E_k, D), \tag{24}$$

$$R(X_2, E_k, D) = [Q_a(E_k, D) + Q_r(E_k, D)]\ R(X_2^+, E_k) \tag{25}$$

$$Q_{r,a}(E_k, D) = \sum_{\mu^+\nu^+J^+} \sum_{\mu\nu J} W(\mu^+\nu^+J^+)\ P_{r,a}(\mu^+\nu^+J^+ \rightarrow \mu\nu J)\ \delta[D(\mu\nu J)-D] \tag{26}$$

and P_t is the probability that an X atom produced by Reaction (3) will reach the surface and be de-excited and thermalized. The factor of 2 in Eq. (24) arises from the stoichiometric factor of Eq. (3). Also, $R(X_2, E_k, D)$ is assumed to be continuous with respect to D.

For the case of low initial impact energy, the product $M_\alpha X_\beta$ is formed only within the first few monolayers, so that analytical measurements can be assumed to be able to sample the full thickness of the layer. Disregarding attenuation of the measurement by outer layers, the intensity $I(E_k, R)$ is then proportional to the number of stoichiometric units formed,

$$I(E_k, R) = Kn(R). \tag{27}$$

Here, $n(R)$ is the number of $M_\alpha X_\beta$ units formed within the reaction volume (defined by the surface layer thickness and area A of the beam) by a dose $R(X, E_k)$ of X atoms received by the surface area A from Process (4). The proportionality constant K contains the relevant instrumental factors and probability function of the analytical measurement.

The relation of $n(R)$ to $R(E_k, X)$ can be obtained by solving the differential equation

$$dn(R) = [n(M) - \alpha n(R)]\, \sigma(X)/A\, dR, \tag{28}$$

where $n(M)$ is the number of target atoms M in the reaction volume of the clean surface, and $\sigma(X)$ is the reaction cross section of X atoms with lattice atoms M. Rearranging Eq. (28), we can write

$$d[n(M) - \alpha n(R)] = [n(M) - \alpha n(R)] \left[-\frac{\alpha\sigma(X)}{A}\right] dR, \tag{29}$$

and upon direct integration we obtain

$$n(R) = \frac{n(M)}{\alpha} (1 - \exp(-\alpha\sigma(X)R/A)). \tag{30}$$

For low doses of X_2^+ ions and low impact energies, we have $\sigma(X)\, R(X)/A \ll 1$. Under this condition we can expand Eq. (30) and safely retain only the

the first two terms to obtain

$$n(R) = n(M)\sigma(X)R(X)/A. \tag{31}$$

Substituting Eqs. (24) - (26) and (31) into (27), we have

$$I(E_k, R) = [C_a G_a(E_k) + C_r G_r(E_k)]\, R(X_2^+, E_k) \tag{32}$$

where $C_z = Kn(M)\sigma(X)P_t\bar{A}_z \qquad z = r, a$ (33)

and

$$G_z(E_k) = \int_0^{E_k} P(E_k, D)\, Q_z(E_k, D)dD. \tag{34}$$

3. Remarks

A simple quantum mechanical model is constructed to provide qualitative understanding of the detailed steps involved in the reaction of low-energy ($\lesssim$ 30 eV) homonuclear diatomic ion beams with metal surfaces. In this model, all the dynamical information is contained in the two adjustable parameters C_a and C_r [see Eq. (33)]. The theoretical calculations involve the evaluation of the band structure of the metal, the Franck-Condon factors and the Hönl-London factors of cations and molecules. In addition, it has been shown that the electronic structure of the metal, cations and molecules are initial factors in determining low-energy nitridation of a metal surface by N_2^+.[7]

The present model neglects the Auger de-excitation process of the projectiles which are neutralized by the resonant process. Nevertheless, since both of the electronic matrix elements of the Auger and the resonant processes are left as adjustable parameters, this assumption

does not affect the model. On the other hand, the neglect of the electronic interaction between the metal surface and the cations/ molecules, which alters the equilibrium distances of the cations and the molecules and the electronic and vibrational energy levels, might introduce some error in the computation of the Franck Condon and Hönl-London factors.

B. Eley-Rideal-Type Reaction: O(g) + C-Pt(111)

Bombarding oxygen atoms on a carbon-platinum adspecies-surface system has been studied by Tully[8] with a stochastic trajectroy technique, where only direct (Eley-Rideal-type) reactive encounters are simulated. The interaction potential is taken to be the London-Erying-Polyani-Sato (LEPS) form[9] with empirical parameters. The potential incorporates experimental information about the gas-phase CO molecule and about C, O and CO absorbed on Pt(111). A brief account of the stochastic formalism is given below.

1. Generalized Langevin Equation

In the situation that localized reaction events take place in the midst of very large assemblies of atoms, the stochastic trajectory technique can be used to eliminate the vast majority of "uninteresting" atoms and to focus on the local region of action. The objective of the stochastic trajectory approach is to accurately describe the flow of energy into and out of the local region of action without explicit inclusion of huge numbers of uninteresting atoms.

The method discussed here, as used recently by Tully,[9] is based on the pioneering work of Adelman and Doll.[10] There are two basic assumptions in the method. The first is that the solid is harmonic,

such that the mass-weighted coordinates u_i of the atoms in the solid satisfy the equation

$$\ddot{\underset{\sim}{u}}_i(t) = \sum_{j=1}^{N} \underset{\approx}{\Omega}^2_{ij} \underset{\sim}{u}_j(t), \tag{35}$$

or in matrix notation,

$$\ddot{\underset{\sim}{u}}(t) = - \underset{\approx}{\Omega}^2 \underset{\sim}{u}(t), \tag{36}$$

where

$$\Omega^2_{ij} = (m_i m_j)^{-1/2} K_{ij}, \tag{37}$$

m_i is the mass of the atom in the solid, and K_{ij} is the force constant.

The second assumption is that the forces experienced by the gas atoms depend on the instantaneous positions of only a small number, n, of local surface atoms. We designate these as the "primary lattice atoms". The remaining N-n solid atoms serve as a heat bath for the incident gas atom and the primary lattice atoms. These are "secondary lattice atoms". One can introduce the projection operators $\hat{P}$ and $\hat{Q}$ which, respectively, project onto the primary lattice and the secondary lattice atoms. The operators have the usual projection properties

$$\hat{P} + \hat{Q} = 1; \quad \hat{P}^2 = \hat{P}; \quad \hat{Q}^2 = \hat{Q}; \quad \hat{P}\hat{Q} = 0. \tag{38}$$

Using these properties, we can partition Eq. (35) to yield

$$\ddot{\underset{\sim}{u}}_P(t) = -\underset{\approx}{\Omega}^2_{PP} \underset{\sim}{u}_P(t) - \underset{\approx}{\Omega}^2_{PQ} \underset{\sim}{u}_Q(t) \tag{39}$$

$$\ddot{\underset{\sim}{u}}_Q(t) = -\underset{\approx}{\Omega}^2_{QP} \underset{\sim}{u}_P(t) - \underset{\approx}{\Omega}^2_{QQ} \underset{\sim}{u}_Q(t), \tag{40}$$

where

$$\underset{\sim}{u}_P(t) = \hat{P}\underset{\sim}{u}(t), \quad \underset{\approx}{\Omega}^2_{PQ} = P\underset{\approx}{\Omega}^2 Q, \text{ etc.} \tag{41}$$

In the presence of the gas-phase atoms, the equations of motion of the gas atoms, primary and secondary atoms are given by

$$\ddot{\underset{\sim}{x}}(t) = \underset{\sim}{F}_x[\underset{\sim}{x}(t), \underset{\sim}{u}_P(t), \bar{\underset{\sim}{u}}_Q] \tag{42}$$

$$\ddot{\underset{\sim}{u}}_P(t) = - \underset{\approx}{\Omega}^2_{PP}\underset{\sim}{u}_P(t) - \underset{\approx}{\Omega}^2_{PQ}\underset{\sim}{u}_Q(t) + F_P[\underset{\sim}{x}(t), \underset{\sim}{u}_P(t), \bar{\underset{\sim}{u}}_Q] \tag{43}$$

$$\ddot{\underset{\sim}{u}}_Q(t) = - \underset{\approx}{\Omega}^2_{QP}\underset{\sim}{u}_P(t) - \underset{\approx}{\Omega}^2_{QQ}\underset{\sim}{u}_Q(t) \tag{44}$$

where $\underset{\sim}{x}(t)$ are the mass-weighted coordinates of the gas atoms. F_x and F_P are mass-weighted forces, derived from the gas-surface interaction potential U by

$$F_{x_i}[\underset{\sim}{x}(t), \underset{\sim}{u}_P(t), \bar{\underset{\sim}{u}}_Q] = - \frac{\partial U}{\partial x_i}[\underset{\sim}{x}(t), \underset{\sim}{u}_P(t), \bar{\underset{\sim}{u}}_Q] \tag{45}$$

$$F_{P_i}[\underset{\sim}{x}(t), \underset{\sim}{u}_P(t), \bar{\underset{\sim}{u}}_Q] = - \frac{\partial U}{\partial u_{P_i}}[\underset{\sim}{x}(t), \underset{\sim}{u}_P(t), \bar{\underset{\sim}{u}}_Q]. \tag{46}$$

Note that the forces only depend on the equilibrium positions $\bar{\underset{\sim}{u}}_Q$ of the secondary lattice atoms.

We can write a formal solution of Eq. (44) as

$$\underset{\sim}{u}_Q(t) = \underset{\sim}{u}^0_Q(t) - \int_0^t dt' \underset{\approx}{G}(t, t')\underset{\approx}{\Omega}_{QP}\underset{\sim}{u}_P(t'), \tag{47}$$

where $\underset{\sim}{u}^0_Q(t)$ is the homogenous solution given by

$$\underset{\sim}{u}^0_Q(t) \equiv \cos(\underset{\approx}{\Omega}_{QQ}t)\underset{\sim}{u}^0_Q(0) + \underset{\approx}{\Omega}^{-1}_{QQ} \sin(\underset{\approx}{\Omega}_{QQ}t)\ \underset{\sim}{u}^0_Q(0). \tag{48}$$

Choosing the Dirichlet boundary condition, the Green's function can be expressed as

$$\underset{\sim}{G}(t, t') = \underset{\sim}{\Omega}_{QQ}^{-1} \sin[\underset{\sim}{\Omega}_{QQ}(t-t')]. \tag{49}$$

Substituting Eqs. (48) and (49) into (47), we obtain

$$\underset{\sim}{u}_Q(t) = \cos(\underset{\sim}{\Omega}_{QQ}t)\ \underset{\sim}{u}_Q(0) + \underset{\sim}{\Omega}_{QQ}^{-1} \sin(\underset{\sim}{\Omega}_{QQ}t)\ \dot{\underset{\sim}{u}}_Q(0)$$

$$-\int_0^t dt' \underset{\sim}{\Omega}_{QQ}^{-1} \sin[\underset{\sim}{\Omega}_{QQ}(t-t')]\underset{\sim}{\Omega}_{QP}^{-2}\ \underset{\sim}{u}_P(t'). \tag{50}$$

Upon integration by parts, Eq. (50) becomes

$$\underset{\sim}{u}_Q(t) = \cos(\underset{\sim}{\Omega}_{QQ}t)\ \underset{\sim}{u}_Q(0) + \underset{\sim}{\Omega}_{QQ}^{-1} \sin(\underset{\sim}{\Omega}_{QQ}t)\ \dot{\underset{\sim}{u}}_Q(0)$$

$$- \underset{\sim}{\Omega}_{QQ}^{-2}\ \underset{\sim}{\Omega}_{QP}^{2}\ \underset{\sim}{u}_P(t) + \underset{\sim}{\Omega}_{QQ}^{-2} \cos(\underset{\sim}{\Omega}_{QQ}t)\ \underset{\sim}{\Omega}_{QP}^{2}\ \underset{\sim}{u}_P(0)$$

$$+ \int_0^t dt' \underset{\sim}{\Omega}_{QQ}^{-2} \cos[\underset{\sim}{\Omega}_{QQ}(t-t')]\ \underset{\sim}{\Omega}_{QP}^{2}\ \dot{u}_P(t'). \tag{51}$$

Substituting Eq. (31) into (43) one obtains the Generalized Langevin Equation (GLE):

$$\ddot{\underset{\sim}{u}}_P(t) = - \underset{\sim}{\Omega}_{eff}^{2}\ \underset{\sim}{u}_P(t) - \underset{\sim}{\Lambda}(t)\ \underset{\sim}{u}_P(0) - \int_0^t dt' \underset{\sim}{\Lambda}(t-t')\ \dot{\underset{\sim}{u}}_P(t')$$

$$+ \underset{\sim}{R}(t) + \underset{\sim}{F}_P(\underset{\sim}{x}(t), \underset{\sim}{u}_P(t), \overline{\underset{\sim}{u}}_Q), \tag{52}$$

where

$$\underset{\sim}{\Omega}^2_{eff} = \underset{\sim}{\Omega}^2_{PP} - \underset{\sim}{\Lambda}(0) \tag{53}$$

$$\underset{\sim}{\Lambda}(t) = \underset{\sim}{\Omega}^2_{PQ}\ \underset{\sim}{\Omega}^{-2}_{QQ}\ \cos(\underset{\sim}{\Omega}_{QQ}t)\ \underset{\sim}{\Omega}^2_{QP} \tag{54}$$

$$\underset{\sim}{R}(t) = -\underset{\sim}{\Omega}^2_{PQ}\ \underset{\sim}{u}^0_Q(t). \tag{55}$$

Since the time dependent of $\underset{\sim}{u}^0_Q(t)$ is influenced by the motion of the primary atoms, the term $\underset{\sim}{R}(t)$ behaves like an external force in Eq. (52). Furthermore, the initial conditions $\underset{\sim}{u}_Q(0)$ and $\dot{\underset{\sim}{u}}_Q(0)$ are not known precisely and are randomly distributed for a given temperature. Therefore, $\underset{\sim}{R}(t)$ can be taken as a random force, and because of the random impulses injected by $\underset{\sim}{R}(t)$, the trajectories are termed "stochastic".

The above GLE is exact, but the friction kernel $\underset{\sim}{\Lambda}(t)$ and the random force $\underset{\sim}{R}(t)$ are very complicated. Exact evaluation of Eq. (52) would involve the same labor as solving the original enormous set of Eqs. (43) and (44). The objective of the GLE approach is to approximate $\underset{\sim}{\Lambda}(t)$ and $\underset{\sim}{R}(t)$ in such a way that they are easy to compute and yet adequately describe the effects of the heat bath on the primary lattice atoms. First, $\underset{\sim}{R}(t)$ can be represented by a Gaussian random force due to the assumption of the harmonic motion of the secondary lattice atoms. Second, the autocorrelation function of $\underset{\sim}{R}(t)$ is related to the friction kernel $\underset{\sim}{\Lambda}(t)$ by means of the "second fluctuation-dissipation theorem,"[11]

$$\langle \underset{\sim}{R}(t)\ \underset{\sim}{R}^+(0) \rangle = k_B T \underset{\sim}{\Lambda}(t), \tag{56}$$

where T is the temperature of the lattice and k_B is the Boltzmann's constant. Qualitatively, it states that the energy dissipated from

the primary zone by the friction must balance the energy introduced by the fluctuating force in order to maintain a certain temperature T. Eq. (56) provides us with a prescription for constructing $\underset{\sim}{R}(t)$ as long as $\underset{\sim}{\Lambda}(t)$ has been determined; thus simulations can be performed at any desired temperature, no matter how small the primary zone. In the actual computation, the friction kernel $\underset{\sim}{\Lambda}(t)$ is usually modelled phenomenologically; more precisely, a simple expression is employed for $\underset{\sim}{\Lambda}(t)$ with some adjustable parameters such that the surface and the bulk properties can be best reproduced. For example, $\underset{\sim}{\Lambda}(t)$ can be expressed as the solution of the damped harmonic-oscillator differential equation, given by

$$\underset{\sim}{\Lambda}(t) = \underset{\sim}{A} \exp(-\underset{\sim}{\gamma} t + i \sqrt{\underset{\sim}{\omega}^2 - \underset{\sim}{\gamma}^2}\, t), \tag{57}$$

where γ_{ij} is the damping coefficient and ω_{ij} is the harmonic frequency. Thus, the elements of the three matrices $\underset{\sim}{A}$, $\underset{\sim}{\gamma}$ and $\underset{\sim}{\omega}$ are chosen to best reproduce known experimental or theoretical information about the surface vibrations of a lattice.

2. Potential Energy Hypersurface

The interaction potential is the most uncertain and also the most crucial ingredient to this study. An empirical interaction potential, as mentioned above, of the LEPS form,[12] based on experimental information about the isolated CO molecule and about C, O and CO adsorbed on Pt(111), can be employed. However, due to limited experimental information, there is a large uncertainty associated with this procedure. Nevertheless, the interaction potential can be varied by adjustable

parameters such that gross qualitative features of the reaction dynamics are elucidated.

The main interest in the present reaction is the energy disposal of the exothermicity. The binding energy of carbon atom to Pt(111), which directly affects the exothermicity of the reaction, is probably the most uncertain feature of the interaction potential. Reasonable values for the C-Pt(111) binding energy range from 4.0 to 7.5 eV, corresponds to reaction exothermicities of 7.6 to 4.1 eV. For this reason, the empirical parameters of the interaction potential are varied such that the exothemicity changes substantially from 6.1 to 3.8 eV, where it is seen that gross features of the reaction dynamics have little dependence on the magnitude of the exothermicity.

3. Results and Remarks

The reaction of the gas-phase oxygen atom with carbon absorbed on platinum(111) has been simulated in the following way: oxygen is directed normal to the surface with the two fixed initial kinetic energies, 2 and 10 kcal/mole, at an initial distance of 12 Å away from the surface. Two different surface temperatures, 0 and 500° K, are examined. In all cases studied, the reaction probability of forming a CO molecule is very high. This is no surprise, since there is no potential barrier in the interaction potential. Furthermore, most CO molecules escape from the surface within a few picoseconds. A large percentage of the liberated energy is disposited in the gas-phase CO molecule, partitioned among translations, vibrational, and rotational degrees of freedom. The rotational motion is formed to be anisotropic, i.e., molecules tend to tumble rather than rotate in the plane of the

surface. The angular distribution is broad and is biased toward the normal direction. Significant alterations of the interaction potential can result in a change of the partition of the energy among translation, vibration and rotation of the CO molecules.

In the present study, the energy has been assumed to flow to and from vibrational modes of the solid. However, contributions from electronic excitation and de-excitation within the solid have not been accounted for. This may introduce substantial error in the present reaction, since platinum is a metal possessing conduction electrons that can be easily excited. Also, possible quantum effects such as vibrational adiabaticity,[13] which is important in gas-phase reactions, have not been considered.

III. RECOMBINATION

Atomic recombination dynamics of the H_2 + W(001) system have been investigated by McCreery and Wolken[14] with a model potential[15] of the LEPS form. The process involves: (i) initial adsorption of the hydrogen as atoms on the surface, (ii) possible equilibration, and (iii) recombination and description of the hydrogen molecule. This sequence is known as the Langmuir-Hinshelwood process. The model assumes that the surface is rigid, which means that there is no energy transfer between the atom and lattice. The assumption should be valid when the absorption time and the recombination and description times are much shorter than the absorbate-surface vibrational relaxation time.

In this section, we will consider the following issues: (i) the formation of the rigid surface potential, (ii) the extention to the moving surface model with the lattice dynamics described by the Einstein model; and (iii) comparison of the Einstein model with the GLE for different values of macroscopic parameters.

A. Rigid Surface Model Potential

The LEPS potential is derived from a valence bond treatment for a system of three one-electron atoms. For the problem of a diatom AB colliding with a solid surface, there are also three two-body interactions of interest: atom A-surface, atom B-surface and atom A-atom B. Due to the infinite extent of the solid, the interbody separations are subjected to fewer geometrical constraints than the three-atom case, and a new asymptotic limit is introduced where both atoms are near the surface but the A-B interatomic distance is large.

The energy expression for the four-electron four-orbital valence bond structure is given by[16]

$$E = Q_{ab} + Q_{cd} + Q_{ac} + Q_{bd} + Q_{cb} + Q_{ad}$$
$$- \{\tfrac{1}{2}[(\alpha - \beta)^2 + (\gamma - \alpha)^2 + (\beta - \gamma)^2]\}^{\frac{1}{2}} \tag{58}$$

where Q_{ij} is the Coulombic energy for the two-electron system i-j, and

$$\alpha = \alpha_1 + \alpha_2 \qquad \alpha_1 = (ab), \qquad \alpha_2 = (cd)$$
$$\beta = \beta_1 + \beta_2 \qquad \beta_1 = (ad), \qquad \beta_2 = (bc) \tag{59}$$
$$\gamma = \gamma_1 + \gamma_2 \qquad \gamma_1 = (ac), \qquad \gamma_2 = (bd)$$

are exchange integrals for the two centers indicated. More precisely,

$$(ab) = \langle abcd|H|bacd\rangle, \text{ etc.} \tag{60}$$

For the case of a diatomic molecule interacting with a solid surface, the valence bond energy formula is modified such that the solid can provide the electrons for bonding to the incident atoms at any point (or points) on the surface. Therefore, a simple model of chemisorption is obtained by only considering those structures describing a-b, a-d, and b-c interactions. This leads to the energy expression

$$E = Q_{ab} + Q_{ad} + Q_{bc} - \{\tfrac{1}{2}[(\alpha_1 - \beta)^2 + \alpha_1^2 + \beta^2]\}^{\frac{1}{2}}. \tag{61}$$

We follow the usual LEPS treatment by assuming that the atom-atom and atom-surface interactions are adequately described by Morse potentials. Additional flexibility is gained by introducing a Sato parameter Δ, which is inserted in such a way as to have no effect when one or more of the distances becomes large. Thus we obtain a diatom-solid potential of the form

$$V = \frac{1}{1+\Delta}\{V_1 + V_2 + V_3 - [A_1^2 + (A_2 + A_3)^2 - A_1(A_2 + A_3)]^{\frac{1}{2}}\} \tag{62}$$

$$\text{where } V_i = \frac{D_i}{4}[(3+\Delta)\exp(-2\alpha_i(r_i-r_{io})) - (2+6\Delta)\exp(-\alpha_i(r_i-r_{io}))] \tag{63}$$

$$A_i = \frac{D_i}{4}[(1+3\Delta)\exp(-2\alpha_i(r_i-r_{io})) + (6+2\Delta)\exp(-\alpha_i(r_i-r_{io}))] \tag{64}$$

and D_i, α_i and r_{io} are the dissociation energy, Morse parameter and equilibrium distance for the i-th two-body interaction. The power of the LEPS method lies not so much in its quantitative description of the potential as in a reasonable description of the potential surface with sufficient flexibility to permit the study of a wide variety of shapes of potentials.

To describe the static periodicity of the solid surface, the dissociation energy and the equilibrium distance of the H-W (001) are written as functions of x and y, which are Cartesion coordinates parallel to the plane of the W (001) surface, given by

$$D(x,y) = D_o[1 + \delta\, Q(x,y)], \tag{65}$$

$$r_o(x,y) = Z_m[1 + \varepsilon\, P(x,y)]. \tag{66}$$

Q(x,y) and P(x,y) are chosen to have the correct symmetry for the W (001) surface and enough adjustable parameters to fit the Extended Hückel Molecular Orbital (EHMO) computed points[17] for the three possible binding sites, 1CN, 2CN and 5CN, on the surface. The numbers 1, 2 and 5 correspond to the number of tungsten surface atoms coordinated to the adsorbed hydrogen atom. Thus, Q(x,y) takes the simple form

$$Q(x,y) = \cos(\frac{2\pi x}{a}) + \cos(\frac{2\pi y}{a}) - A[\cos(\frac{2\pi x}{a}) - 1][\cos(\frac{2\pi y}{a}) - 1] \ , \qquad (67)$$

where "a" is the 1CN separation. Given that D_o is the dissociation energy at the 2CN site, δ is then determined by the binding energy at a 1CN site and D_o, and A is determined by the binding energy at a 5CN site and δ. P(x,y) takes a form similar to Eq. (67) but with constants determined from the equilibrium heights above the 1CN, 2CN and 5CN positions.

B. Moving Surface Model Potential

The rigid surface potential, V_{LEPS}, described above can be generalized to a moving surface model by introducing two correction terms:

(1) V_R, the restoring force on each atom of the solid, tending to return it to its lattice site;

(2) V_{CORR}, to account for the change in the gas-surface interaction when the solid atom is displaced from its lattice site.

Thus, we have

$$V_{Total} = V_{LEPS} + V_R + V_{CORR}. \qquad (68)$$

There are two basic assumptions in this model. First, there is only a small number of moving surface atoms. Second, the Einstein model[18] is used to describe the restoring force of the moving surface atoms, whereby V_R is represented by a harmonic potential binding an atom of the solid to its (fixed) lattice site. On the other hand, Morse potentials for V_{CORR} connecting each gas atom with each surface atom are used to account for the change in the gas-solid potential due to displacement of the surface atom from its lattice site. However, V_{LEPS} already contains the interaction of each gas atom with each lattice site. To avoid including it twice, this lattice site interaction must be substracted from V_{CORR}, so that

$$V_{CORR} = \sum_{g}^{N_g} \sum_{s}^{N_s} [W(R_{g-s}) - W(R_{g-1})], \tag{69}$$

where N_g is the number of gas atoms, N_s is the number of moving surface atoms, and R_{g-s} is the distance between the gas atom and the lattice site of the solid atom. As required, if the moving surface atom occupies its lattice site, i.e., $R_{s-g} = R_{s-1}$, then $V_{CORR} = 0$. The total gas-solid potential for the moving surface case is then

$$V_{Total} = V_{LEPS} + \sum_{s}^{N_s} V_R^2 + \sum_{g}^{N_g} \sum_{s}^{N_s} [W(R_{g-s}) - W(R_{g-1})], \tag{70}$$

where V_R^s is the harmonic restoring force for the moving surface atoms.

McCreery and Wolken[19] have used this moving surface model to examine the validity of the rigid surface approximation for the recombination dynamics of H_2 + W (001). Out of 100 trajectories, only a small percentage of the total energy available to the product molecules is transferred between the gas atoms and the surface atoms. Furthermore, the energy distribution of the escaping molecules is very similar for both the rigid surface and the moving surface. However, the amount of recombination for the moving surface is about twice as large as for the rigid surface. This suggests the inadequacy of the rigid surface representation for describing the recombination dynamics. An unanswered question is the accuracy of the Einstein model. To fully address the problem, a complete lattice dynamics calculation, such as with the GLE, is required to justify the Einstein model and the rigid surface assumption.

C. Comparison of the Einstein Model with the Generalized Langevin Equation for Different Macroscopic Parameters

Diebold and Wolken[29] studied the energy accomodation and dissociative adsorption of diatomic-surface scattering on a LEPS-type potential with two different methods. One is the GLE approach described in Sec. II, but with an additional approximation: the friction kernel $\Lambda(t)$ is approximated by a single-term damped cosine function obtained by a numerical fit to a modified bulk Debye model of the solid. The other method is the Einstein model approach, which simply replaces the friction kernel and the random force by a single oscillator. The interaction potential was taken to be the form of Gelbs and Cardillo[21] describing the interaction of H_2 with Cu (001). The hydrogen-copper potential parameters were chosen to be those of Gregory et al.[22]

Two different collison configurations - one that leads to dissociative adsorption and one that does not - were examined for different solid temperatures, Debye temperatures and atomic masses. For the latter collision configuration, one restricts the bond axis of the molecule to be perpendicular to the plane of the surface and positions the incoming molecule directly over the struck solid atom. Here the energy exchange is directly analyzed without any complication due to multiple collisions with the surface and diatom rotational dynamics. The internal energy of the diatom was chosen to be the same as that of the ground vibrational and rotational state of the hydrogen molecule. For a fictitions hydrogenic molecule composed of atoms twenty times as massive as a hydrogen atom, the amount of energy transfer is seen to decrease slowly with increasing solid temperature for both the

single-oscillator and GLE approaches. However, the results of the GLE approach are generally found to be twice as large as those of the single-oscillator approach. Increasing the Debye temperature, at a fixed solid temperature, the energy exchange is seen to decrease. As before, the results of the single oscillator are too small compared to those of the GLE. For a 300°K solid with the copper Debye temperature, energy transfer of the hydrogen molecule and fictitious molecules with atoms ten times and twenty times the mass of hydrogen were examined. The results of the hydrogen molecule are very similar for both the GLE and single-oscillator approachs, but the agreement starts to deviate as the atomic mass increases.

For the former collision configuration leading to dissociative adsorption, the sticking probabilities were computed as functions of those macroscopic parameters. In all cases studied, the single-oscillator model shows the same trends as the GLE results, but with much smaller sticking probabilities. There are two exceptions: the single-oscillator model converges to the GLE results as the atomic mass decreases or the Debye temperature increases. Thus, one can conclude that the single-oscillator model is a good approximation when the atomic mass is small or the incident velocity is large.

IV. ADSORPTION

Microscopic, dynamical treatments of the adsorptive process are still at an early stage of development, and such treatments that do exist are restricted either to classical trajectory studies using effective potentials, or to highly simplified quantum or semi-classical models. What all these treatments have in common is some mechanism for dissipation of the excess kinetic energy of the incoming particle, and they may be classified accordingly. We list here four important classes of dissipation:

(1) phonon excitation

(2) polarization effects

(3) dissociation

(4) rotational excitation.

[Of these, the last is not strictly dissipative, in the sense of an irreversible decay, but is included for completeness.] There is very little literature on dissociation as a mechanism for dissipation, such as there is being devoted mainly to static problems. We therefore make a survey of work falling into classes (1), (2) and (4).

A. Dissipation by Phonon Excitation

The methodology for the most detailed calculations to date has been the Generalized Langevin Equation,[9,10] which is reviewed in Sec. II of this article. In other words, the most quantitative calculations have been classical treatments using effective (dissipative) potentials. In principle, nothing further needs to be added, since in this instance the unifying concept for all the various kinds of surface process is the

classical trajectory, the only difference between adsorption and desorption, say, being that one trajectory ends where the other begins. It is only in quantum mechanics that different kinds of model are used to treat different processes.

A phenomenological semi-classical treatment has recently been given[23] in which the technology of gas-phase collision theory has been transferred to treat adsorption. The incoming particle is assumed to move on a repulsive potential with respect to the surface and interacts via an avoided crossing with a bound electronic state. The system can therefore form resonances, but the adatom will eventually dissociate. If however the trajectory includes dissipation, then after oscillating a few times in the bound state the particle drops below the crossing point and is effectively adsorbed. The model is a multiple-pass Landau-Zener problem, with dissipation. In the case of no dissipation, the probability of returning out is given by

$$P_{out} = (1-P_{12}) + P_{12}^2 \sum_{n=0}^{\infty} (1-P_{12})^n = 1, \tag{71}$$

where P_{12} is the Landau-Zener probability of switching curves at each pass of the crossing-point. Clearly, what goes in must come out. However, a crude approximation for the dissipation is given by restricting the number of passes to a finite number N. This is calculated by assuming a constant decay rate $\frac{\Gamma}{\hbar}$, that is, a constant rate of decaying below the crossing-point. Then the time taken to decay is just $t = \frac{\hbar}{\Gamma}$, and the number of passes that occur before this happens is just

$$N = \nu t = \frac{\pi\nu}{\Gamma} , \tag{72}$$

where ν is the vibrational frequency of the bound motion. It is clear that this phenomenological treatment is quite limited unless values for P_{12} and Γ are known. This would in general be the most difficult part of the problem. However, there is a more severe limitation on this kind of treatment for phonon dissipation, namely an implicit assumption of weak coupling. When the coupling is strong it is impossible to separate the motion of the adatom from the motion of the surface. Consequently, a proper representation must in general go beyond such a simple two-body Landau-Zener treatment, in which the many-body aspects have been bundled into a phenomenological width term. We note, however, that the above treatment is so general that it could be applied to problems with completely different mechanisms of dissipation.

B. Dissipation by Excitation of Electron-Hole Pairs

The phenomenon of dissipation by polarization effects is particularly appropriate for deposition on metal surfaces, where such effects are large. This class would include for example dissipation due to plasmon excitation. However, in the following we restrict ourselves to a discussion of electron-hole pair formation.

We now consider the process by which an adatom couples with the bulk electrons of a metal causing excitation of the substrate. The literature on this effect is very extensive[24-33] and is based mostly on the semi-classical Anderson model,[25] although there have recently been attempts to introduce fully quantum descriptions.[24,33] We shall describe the

semi-classical treatments. The overall process is one of considerable complexity and consequently all treatments to date have made extensive use of models and approximations. The essential idea is that an atom approaching a surface causes a time-varying perturbation which can promote electrons near the Fermi surface to excited states, thereby creating electron-hole pairs. As a result, the atom may lose an amount of kinetic energy sufficient to allow it to stick. It is assumed throughout that the atom maintains its character even in the vicinity of the surface and does not form a chemical bond. The descriptions therefore are limited to theories of physisorption. Moreover, only the attractive part of the interaction potential contributes to electron-hole pair formation, it is being assumed that in the repulsive region phonon excitation is the dominant dissipative mechanism.[34] It is implicitly assumed also that the electrons interact with the adsorbate by means of a local potential. Among other things, this means physically that individual excitation events are independent. Therefore, the total probability for adsorption can be obtained by summing the probabilities of all events that can lead to adsorption.

The model is not fully consistent since the trajectory of the adatom is calculated on the assumption that no energy is lost. In practice, however, this approximation is not expected to be severe since the strongest interaction occurs where the local velocity is very much larger than the initial velocity. Consequently, the change in velocity due to the substrate excitations is expected to be relatively small. Finally, the semi-classical approximation will break down where the classical trajectory is an

inappropriate description of the nuclear motion, that is, for light adatoms at low collision energies.

The central quantity to be calculated is the probability $P_{\varepsilon'}(\varepsilon)$ that an incoming particle with energy ε' loses energy ε to the substrate during one round trip. We assume that the substrate is initially in a state denoted by $|\varepsilon_1\alpha_1>$, where ε_1 is the energy and α_1 is a set of quantum numbers (such as polarization, spin, etc.) which complete the description. The entire treatment may be given in terms of standing wave states since the Born approximation to the electron scattering is applied. Furthermore, let us assume that the time dependence of these states is given by a coefficient $c_{\varepsilon_1\alpha_1}(t)$. Then we can write[35]

$$c_{\varepsilon_2\alpha_2}(\infty) = -\frac{i}{\hbar}\int_{-\infty}^{+\infty} dt V_{12}(t) e^{i(\varepsilon_2-\varepsilon_1)t/\hbar}, \tag{73}$$

where $V_{12}(t) = <\varepsilon_2\alpha_2|V(t)|\varepsilon_1\alpha_1>$,

and V is the interaction due to the adatom. Integrating by parts, using $V_{12}(-\infty) = 0$, we obtain

$$c_{\varepsilon_2\alpha_2}(\infty) = \int_{-\infty}^{+\infty} dt \frac{<\varepsilon_2\alpha_2|V(t)|\varepsilon_1\alpha_1>}{\varepsilon_2 - \varepsilon_1} e^{i(\varepsilon_2-\varepsilon_1)t/\hbar}. \tag{74}$$

The sticking probability is given by

$$s = \int_{\varepsilon'}^{\infty} d\varepsilon P_{\varepsilon'}(\varepsilon). \tag{75}$$

This means that a particle with energy ε' must lose an amount of energy equal to at least ε' in order to stick. From here on we suppress the subscript ε', it is being assumed that we are considering only these

particles. Then we can write

$$P(\varepsilon) = \sum_{\alpha_1\alpha_2} \iint d\varepsilon_1 d\varepsilon_2 |c_{\varepsilon_2\alpha_2}(\infty)|^2 f(\varepsilon_1)(1-f(\varepsilon_2))\delta(\varepsilon-(\varepsilon_2-\varepsilon_1)), \tag{76}$$

where f is the Fermi-Dirac distribution. In other words, the excitation can only take place if the initial state is occupied and if the final state had been vacant. A very useful form for the matrix element in Eq. (74) appears in the Born approximation. That is, if the states of the electronic substrate are represented as ordinary (time-independent) plane wave states, then we can write it in terms of the Born approximation T-matrix

$$\langle\varepsilon_2\alpha_2|\hat{V}(t)|\varepsilon_1\alpha_1\rangle = \frac{\partial}{\partial t} T(\varepsilon_2\alpha_2;\varepsilon_1\alpha_1). \tag{77}$$

Furthermore, let us assume that significant transitions occur only at the Fermi energy, and that the difference between ε_1 and ε_2 is negligible. Then

$$\langle\varepsilon_2\alpha_2|\hat{V}(t)|\varepsilon_1\alpha_1\rangle \sim \frac{\partial}{\partial t} T(\varepsilon_F\alpha_2;\varepsilon_F\alpha_1), \tag{78}$$

where ε_F is the Fermi energy.

It is always possible to choose a representation which is diagonal in α_1 and α_2. The matrix element in this adiabatic representation is given by $\frac{\partial}{\partial t} T(\varepsilon_F\alpha;\varepsilon_F\alpha)$. However, we can write

$$S = 1 - 2\pi i T = e^{2i\delta_{\varepsilon_F,\alpha}} \approx 1 + 2i\delta_{\varepsilon_F,\alpha}, \tag{79}$$

where $\delta_{\varepsilon_F,\alpha}$ is the elastic scattering phase shift and the approximation is for weak coupling. Hence

$$\langle \varepsilon_2 \alpha_2 | \hat{V}(t) | \varepsilon_1 \alpha_1 \rangle \approx -\frac{1}{\pi} \dot{\delta}_{\varepsilon_{F,\alpha}} . \tag{80}$$

Thus

$$c_{\varepsilon_2 \alpha_2}(\infty) \approx \delta_{\alpha_1 \alpha_2} \frac{1}{\varepsilon} \int_{-\infty}^{\infty} dt \left(-\frac{\dot{\delta}_{\varepsilon_{F,\alpha}}}{\pi} \right) e^{i\varepsilon t} , \tag{81}$$

where

$$\varepsilon = \varepsilon_2 - \varepsilon_1 . \tag{82}$$

The interaction between the adatom and substrate will be greatest as the energy of the atomic level approaches ε_F. Then the elastic scattering of electrons is dominated by the resonant interaction with the one-particle adatom state. Under these circumstances the phase shift is given by[36]

$$\delta_{\varepsilon_F \alpha}(t) = \tan^{-1} \left[\frac{\Gamma(t)}{\varepsilon_F - \varepsilon_a(t)} \right] = \tan^{-1} \frac{\Gamma(t)}{\Delta(t)} , \tag{83}$$

where $\Gamma(t)$ is the width of the adatom level and ε_a the real part of its energy. Notice that as the energy of the level crosses the Fermi energy, the phase shift varies from $\frac{\pi}{2}$ to $-\frac{\pi}{2}$.

We made two further assumptions. First, Γ is roughly constant during the traversal of the Fermi surface. We therefore set $\Gamma(t) = \Gamma(t_0)$, where t_0 is the time of the crossing. Second, Δ is a linear function of time (this is analogous to one of the Landau-Zener approximations). We then have

$$\dot{\delta}_{\varepsilon_{F\alpha}}(t) = \frac{\partial}{\partial t} \tan^{-1} \frac{\Gamma(t_0)}{\Delta(t)} = -\frac{\Gamma(t_0)}{\Delta^2} \frac{\dot{\Delta}}{1+(\Gamma^2/\Delta^2)} = \frac{(\Gamma/\dot{\Delta})}{\left(\frac{\Delta}{\dot{\Delta}}\right)^2 + \left(\frac{\Gamma}{\dot{\Delta}}\right)^2} . \tag{84}$$

Hence

$$\dot{\delta}_{\varepsilon_F^\alpha}(t) = \frac{\tau}{(t-t_o)^2 + \tau^2} \quad , \tag{85}$$

where τ is the time taken for the system to pass the crossing point (that is, for the phase shift to change by π). Notice that this is a Lorentzian function of the time, which is not surprising since it has been derived for the case of resonance elastic scattering. This form for $\dot{\delta}$ can now be substituted back into Eq. (81) and the sticking probability calculated using Eq. (76).

A related approach[30,31] treats the electronic excitations as bosons and finds solutions to the Heisenberg equations of motion of the occupation numbers. This leads to a simplified form for $P(\varepsilon)$ but appears at first glance to be an unwarranted assumption, except in the case of weak coupling. However, it has been demonstrated that the form holds even for strong coupling,[27] provided the electron-hole pair is treated as a Tomonaga boson.[37]

Realistic calculations of $P(\varepsilon)$ show that systems which undergo a rapid crossing of the Fermi level lend to stick better than systems which make the traversal more slowly.[28] At the opposite extreme are systems which do not undergo any crossing, that is, systems for which the unfilled adatom levels are far removed from the Fermi surface at all points on the trajectory. Thus the rare gas atoms, which have filled shells, stick much less readily by this mechanism, and it is likely that adsorption is due to phonon dissipation. In general, however, it is necessary to consider both electronic and phonon dissipative mechanisms.

C. Rotational Trapping

We consider a diatomic molecule approaching a surface in a potential which can support bound states. With no mechanism for dissipation, it will scatter out elastically after colliding with the repulsive part of the surface-molecule potential. However, during this collision it may undergo rotational excitation in the same way as a football which is bounced off a wall. Thus translational energy is converted into rotational energy, and if the loss is sufficient, the molecule drops into a bound state of motion.

R-matrix calculations have been performed, for HD on Pt(111)[38] and HD on Ag(111),[39] to assess the degree of rotationally inelastic scattering. The potentials used are for rigid corrugated surfaces and are of the form

$$V(Z,\theta) = V_0(Z)\ [1 + \beta P_2(\cos\theta)], \tag{86}$$

where Z is the normal distance from the surface to the geometric center of HD, and θ is the polar angle of the molecular axis from the normal to the surface. $V_0(Z)$ is given as a Morse potential. The results are for rotationally elastic scattering as a function of initial translational energy. The trapping, however, is dynamic in the sense that the final state is a scattering state.

V. DESORPTION

When an adsorbed substance leaves the surface in a manner independent of that of its arrival, we may call it desorption as opposed to scattering. As the desorption rate depends on the surface coverage and activation energy as well as the temperature, desorption may be a useful means of identifying and adjusting the surface population and properties of adspecies of interest as well as determining activation energy and surface coverages. Desorption processes thus have fundamental implications to chemical kinetics and molecular dynamics on surfaces.

For desorption to occur, energy needs to be supplied to surmount a barrier, either due to a van der Waals interaction for the case of physisorption or an actual bond for the case of chemisorption. The required energy can be provided by the impact of ions or electrons, by electromagnetic radiation such as a laser (photodesorption), or by thermal heating (thermal desorption). In flash desorption one prepares a gas-solid system in equilibrium, and the barrier is surmounted due to rapid heating of the solid. Isothermal desorption corresponds to suddenly reducing the gas pressure while keeping the solid at a constant temperature. Although desorption is commonly induced by vibrational excitation, it can be accomplished by electronic excitation. We concentrate here on the theory of the former, with a reference to electronic excitation at the end of this section.

The kinetics of desorption is conventionally interpreted in terms of the transition-state theory.[40-43] Here one assumes desorption to proceed via an energetically activated state which exists at the top of

a potential energy barrier. The theory yields the standard Frenkel-Arrhenius formula for the rate of desorption,

$$k = k_o \, e^{-D/k_B T}, \tag{87}$$

where D is the activation energy, k_B is the Boltzmann constant, T is the temperature (the final temperature of the solid for the case of flash desorption), and the preexponential factor k_o ranges typically from 10^7/sec to 10^{15}/sec depending on the system. Although it is often assumed as a first approximation that k_o and D are constants, they in fact vary with the surface coverage due to interaction between adatoms. Furthermore, the Frenkel-Arrhenius formula is found to be valid only over a limited range of temperature. The ultimate goal left for theorists to achieve is to find the rule that governs the dependence of the desorption rate on temperature, surface coverage and other possible factors such as interaction anharmonicity and lattice dynamics. This has to be accompanied by an accurate determination of D and k_o for a given system. Dynamical aspects such as energy and angular distributions of desorbed particles can also be studied. In the following, we briefly review some selected theoretical progress made during the last several years.

A. Classical Theory

Perhaps the most straightforward way of computing the desorption rate within the framework of classical mechanics is to employ the classical trajectory method widely used in molecular dynamics calculations, i.e., to numerically integrate Hamilton's equations for particles in the system with an appropriate distribution of initial positions and momenta

characterized by a given temperature. The immediate difficulty of this method lies in the fact that desorption is a many-body problem, and consequently the number of coupled equations to be integrated is much too large for the method to be of any use. This difficulty, however, can be alleviated by the GLE approach as described in Sec. II, in which only a few surface atoms in the immediate neighborhood of the adatom in question are given a full consideration.

An early attempt at a kinetic description of desorption in the spirit of the GLE approach was made by Kramers.[44] Grimmelmann, Tully and Helfand[45] applied the GLE approach to compute the desorption rate of xenon atom from the (111) surface of a platinum crystal. The primary zone was considered to contain the Xe atom and four nearby Pt surface atoms whose motion was followed in full detail. If the Xe atom moves outside the initially designated primary zone, original primary atoms were switched off and new ones switched on. Desorption was considered to occur when the separation between Xe and the surface is greater than 10Å. The adatom-surface potential is sufficiently weak beyond 10Å that particles entering this region may be assumed to be desorbed. The desorption rate, however, was reported only at a few high temperature values ($\geq$500°K). The difficulty is that, even with the GLE approach, the computation of the desorption rate requires prohibitively large amounts computer time. This is because desorption is fundamentally an infrequent event. Although trajectories leading to desorption must pass over the top of the potential energy barrier, this region in most cases is represented by a "bottleneck" in phase space. Trajectories spend most of

the time wandering in the low-energy region of phase space and almost never reach the bottleneck region. Consequently, desorption is a slow, infrequent event, especially at low temperatures. It therefore is apparent that some technique of efficiently simulating infrequent events needs to be employed in order to successfully describe desorption processes within the framework of the classical Langevin approach.

One such technique, a compensating potential method, was proposed by Grimmelman, Tully and Helfand.[45] In this method, the interaction potential V, which in general depends on the coordinates of the adatom and surface atoms, is separated into two terms, V = W + U, in such a way that U depends only on a single coordinate, the separation between the adatom and the surface. It then is possible to rearrange the problem in such a way that trajectories subject only to the potential W need to be computed for the evaluation of the desorption rate. If one chooses U so that it contains a potential minimum of approximately the same depth as V, then W contains only a shallow minimum. The compensating potential method therefore improves the efficiency of sampling the bottleneck region by effectively replacing the deep minimum in the interaction potential by a shallow minimum. With this technique, the desorption rate of a xenon atom from a platinum surface was computed down to the temperature T ≈ 100°K. The computed rates are seen to be consistent with the Frenkel-Arrhenius formula over the temperature range 100°K $\lesssim$ T $\lesssim$ 500°K. However, as the temperature is increased beyond 500°K, the rates show deviation from this simple formula.

Another way to describe infrequent events is the pseudo-dynamical

Monte Carlo sampling technique. Adams and Doll[46,47] have incorporated this technique into the classical transition-state theory to compute desorption rates. This involves finding the average rate at which particles, thermally distributed at a given temperature, enter the "desorption region" defined by $s \geq q$, where s is the adatom-surface separation and q is an appropriately chosen separation beyond which the adatom-surface potential is sufficiently weak. Since desorption is an infrequent event, it is not practical to numerically integrate Hamilton's equations in order to generate the function $s = s(t)$. The Monte Carlo sampling technique, however, alleviates this difficulty by allowing one to consider "pseudo-dynamics" of adatoms. The technique provides an efficient means of generating averages over a distribution characterized by a given temperature and is most suitable for the description of desorption processes. With this technique it is possible to compute desorption rates, for example, for a wide range of surface coverages. The Monte Carlo transition-state method has been applied[46] to desorption of a helium atom from the (111) surface of xenon with the He-Xe interaction as well as He-He interaction assumed to be given by the Lennard-Jones 6-12 potential. The computed rates reveal a clear dependence on the surface coverage. The rate was found to be an increasing function of the coverage. For example, in passing from the infinite dilute limit to a monolayer coverage, the rate was almost doubled. This is expected because adatom-adatom interactions are mainly repulsive. At high coverages, adatoms tend to force neighboring atoms off the surface, leading to an increase in the desorption rate.

Another interesting feature revealed by the Monte Carlo calculation is that the temperature dependence of the rate shows the existence of a transition temperature $T_c = 30 \sim 40°K$ for He-Xe(111), i.e., the plot of ℓnk vs. T consists of a line whose slope changes at $T = T_c$. This indicates a change in the activation energy D and the preexponential factor k_o at the transition temperature.

Only recently have powerful numerical techniques such as the ones discussed above been introduced to describe desorption processes, thus making possible relatively accurate determination of desorption rates over a wide range of temperatures. It seems, however, that many of the dynamical details of desorption still remain unanswered. It is hoped that the development of a comprehensive theory at a fundamental level as well as of numerical techniques along the line discussed above will lead to a complete understanding of a desorption process.

B. Quantum Mechanical Theory

Quantum mechanically, thermal desorption is pictured as a transition of an adatom from a bound state to a continuum state, with the required energy supplied by the phonon bath of the solid. The kinetics of desorption is essentially determined by a series of transition matrix elements, $H_{mn} = \langle m|H'|n\rangle$, which describes a transition from the m-th state to the n-th state (H' is the interaction Hamiltonian for the adatom-surface). The success of a quantum mechanical theory therefore depends largely on the capability of obtaining accurate eigenfunctions to evaluate the transition matrix elements.

An early quantum mechanical theory of desorption is due to Lennard-Jones, Strachan and Devonshire.[48,49] They chose a Morse potential to represent an adatom-surface atom interaction and evaluated the transition matrix elements accordingly. The Morse potential seems particularly useful here because the corresponding eigenfunctions are known and the matrix elements can be analytically evaluated. In applying their formalism to desorption, however, they have limited their consideration to the case where the activation energy is sufficiently low that a direct transition from the initial bound level to a continuum level can be mediated by a single phonon. The theory therefore is applicable to only a limited number of systems, with a very low activation energy. In addition, their theory is essentially one dimensional in that the motion of the adatom or surface atoms parallel to the surface plays no role.

Bendow and Ying[50] have attempted a generalization of this early theory by considering multiphonon desorption in three dimensions. From a practical viewpoint, the generalization implies a greater number of transition matrix elements to be evaluated. Furthermore, each element is now more complicated because the eigenfunctions depend not only on the adatom surface separation but also on the coordinates parallel to the surface which reflect the periodicity of the lattice structure. Applying their theory to neon desorbed from xenon-covered graphite, they found that the preexponential factor k_o is unusually small, $k_o \sim 10^5$/sec. It was suggested that this may be due to the inherent difference between one-dimensional and three-dimensional models.

Goodman and Romero[51] reported calculations of desorption rates for the systems H on C and He on Ar, Kr, Xe assuming that desorption occurs via a single-phonon transition. They used a three-dimensional quantum mechanical approach and assumed that the adatom-surface interaction is given by a Morse potential with appropriately chosen parameters for each system. In all cases the rate is seen to follow the Frenkel-Arrhenius formula with k_0 ranging from 10^{10}/sec to 10^{13}/sec. Calculations have also been carried out with one-dimensional models. In contrast to the suggestion by Bendow and Ying, however, the one-dimensional and three-dimensional models yielded essentially the same desorption rates.

A simple model of multiphonon desorption was put forth by Garrison, Diestler and Adelman[52] in which a one-dimensional truncated harmonic potential is used to describe the atom-surface interaction, and eigenfunctions are assumed still to be given by those of the untruncated harmonic potential. The transition matrix elements can then be easily evaluated. The rate constant was simply taken as the reciprocal of the time required to reach the continuum. This model was applied to desorption of a xenon atom from a tungsten surface. The calculated desorption rate exhibits Frenkel-Arrhenius behavior and depends on lattice dynamical properties; in particular, it shows an inverse cube dependence on the Debye temperature. Although the desorption rate is expected to depend upon lattice dynamics, unrealistic assumptions made in this model (truncated harmonic potential, harmonic wavefunctions) limit the reliability of calculated data.

Gortel, Kreuzer and Teshima[53] have developed a quantum mechanical

theory based on the rate equation

$$\frac{dn_i(t)}{dt} = - [R_{ci} + \sum_{j \neq l} R_{ji}] n_i + \sum_{j \neq l} R_{ij} n_j + R_{ic} n_c, \tag{88}$$

where n_i is the time-dependent occupation of the i-th bound state, R_{ij} is the rate of transition from the i-th to j-th bound state, and R_{ci} is the transition rate from the i-th bound state into the continuum. The theory applies mainly to systems with low coverage, because non-linear terms that account for the adatom-adatom interaction are not included in Eq. (88). It can be shown that the desorption rate is the smallest eigenvalue of the matrix R_{ij}. The problem then is reduced to finding the R_{ij}, which in turn are determined by the matrix elements H_{ij}. The matrix elements were evaluated exactly, assuming a Morse potential between the adatom and surface. Calculations showed that desorption in weakly coupled systems with many bound states proceeds predominantly through one-phonon cascades. Isothermal desorption rates were calculated for He-LiF, He-NaF, He-graphite, H-NaCl, He-Ar and Xe-W. All the calculated rates were found to behave according to the Frenkel-Arrhenius formula with activation energy approximately equal to the energy of the lowest bound state. Gortel, Kreuzer, Teshima and Turski[54] showed that a further simplification results if the adatom-surface potential allows a large number of bound states such as in the Xe-W system. In this case, the system may be viewed as having a quasi-continuum instead of many discrete bound states. The system may then be considered to perform a random walk through this quasi-continuum rather than cascading

through bound states. The rate equation, Eq. (88), can then be cast into a form in the continuum limit, and from this the Fokker-Planck equation derived. This equation was shown to lead to a relatively simple expression for the desorption rate for the case of a weakly-coupled system.

In computing the desorption rate, one needs to carry out thermal averaging of the square of the transition matrix elements over phonon modes. At this stage, virtually all the theories that describe desorption have used a bulk Debye model for the solid, i.e., it was assumed that phonons that induce desorption of adatoms from a surface are simply those of an infinite solid. However, surface phonon modes may significantly differ from those of solid, and therefore a proper account of such modes should be given. This problem was undertaken by Goldys, Gortel and Kreuzer,[55] who found that surface phonons contribute to desorption two to three times as much as bulk phonons. From this, an effective surface Debye temperature can be deduced, which turns out to be about 0.65 to 0.8 of the bulk Debye temperature.

Despite progress made during recent years, many details of desorption are still uncharacterized. One of the important aspects of desorption not yet totally answered is the dependence of the rate upon surface coverage. Adatom-adatom interactions are often neglected, which makes it difficult to assess the effect of surface coverage on desorption. The relation between the desorption rate and the adatom-surface interaction potential, e.g., the effect of interaction anharmonicity on the desorption rate, still seems unclear. Although calculations of desorption rates for different interaction potentials exist, it appears that no systematic treatment of this problem

has been given. Nevertheless, some accurate calculations of the rates at low coverages over a wide range of temperatures have begun to appear in recent years.

Finally, we mention that desorption can also be induced by electronic transitions, with the use of, say, an electron or photon beam. In order for desorption to be induced by electronic transitions, an electron must be excited to a state with a repulsive potential energy surface. The molecules or ions will then be repelled and rejected from the surface. The main issue here is not the motion of electrons but the nuclear dynamics that follows the electronic excitation. For a detailed treatment of desorption induced by electronic transitions, we refer to Gadzuk.[56] We shall also consider this problem in Sec. VI in terms of surface state excitation within the substrate.

VI. LASER-STIMULATED RATE PROCESSES

Both the phonon[57] and electron[58] spectra of a solid with a surface have energy levels distinct from the bulk levels of an infinite solid. These levels correspond to vibrations or electronic charge density localized in the vicinity of the surface. The introduction of an adspecies on this surface will also produce phonon and electron energy levels related to the adsorptive bond.

Using a laser, the phonon mode of the adsorptive bond could be excited in a selective manner in order to induce desorption, migration and bond-breaking within the adspecies. A thermal non-selective excitation of the surface phonon modes by the laser could also be used to stimulate these dynamical processes, in addition to serving as a means of annealing. In Part A of this section, we shall discuss the laser excitation of these adspecies-surface phonon modes in detail. After this discussion, we shall examine in Part B the effects of laser radiation on the excitation of surface electrons on a semiconductor. It will be shown that such excitation can have a significant influence on the adspecies-surface interaction potential. Part C will demonstrate the importance of including both electrons and phonons in the laser excitation of a metal surface. Finally, in Part D we will discuss the effects on charge transfer between the surface and an adspecies produced by the altered surface charge caused by laser excitation.

A. Adspecies-Surface Vibrational Modes

The vibrational spectrum of an adspecies-surface system can be divided into a number of distinct modes. The active modes of the

adsorptive bond along with intramolecular vibrations of the adspecies are different from the bath modes of the solid. The bath modes in turn can be viewed as having components due to surface and bulk vibrations of the solid. Fig. 1 is a schematic representation of such a spectrum. An active mode (A) is indicated by the highest energy peak; the high-energy bath modes (B) would be those due to surface vibrations; and the low-energy modes (C) are due to the internal vibrations of the solid.

Laser irradiation of the solid surface with a frequency tuned to the active mode will lead to energy transfer to the adsorptive bond. This can produce selective bond breaking between the adspecies and surface or within the adspecies. However, to accomplish this bond breaking, the laser must pump energy into the active mode faster than the vibration is damped by the coupling between the active and bath modes. This vibrational relaxation is characterized by both an energy (T_1) and phase (T_2) process. In addition to this anharmonic coupling to the bath phonon modes, the T_1 and T_2 processes are also effected by vibration-induced migration of the adspecies, substrate-induced thermal fluctuations of the effective dipole of the adspecies, and charge transfer between the surface and the adspecies.

Both a classical model[59] based on the GLE approach and a quantum model based[60] on the Heisenberg-Markov approximation have been used to describe the relaxation process of these adspecies-surface dynamics. The results have shown that for a given anharmonicity of the effective adsorptive potential, given detuning between the laser frequency and the active mode frequency, and given dephasing lifetime, then selective

excitation is confined to a small range of values of the damping factor γ_1 which is associated with T_1 processes. These selective dynamics, on the other hand, are rather insensitive to T_2 processes.

Fig. 2 shows the effects of the energy relaxation rate γ_1 on the amount of selective excitation of the active mode at the expense of the bath modes.[61] As can be seen by the lower curve (E), there is a threshold for γ_1 beyond which essentially all selectivity disappears. Also, low selectivity for short irradiation times followed by enhanced selectivity for large exposure times points to important feedback mechanisms as well as an optimum irradiation time for maximum selectivity.

Despite its importance, values of γ_1 are not easily obtainable from either theory or experiment. A mostly first-principles formulation for γ_1, however, has recently been developed.[62] The relaxation rate is given by the Fermi golden rule for a perturbation which is the difference in the potential due to the lattice atoms at their instantaneous and equilibrium positions. This rate reduces to a sum of products of matrix elements involving only adatom properties and time Fourier transforms of correlation functions for different lattice displacements at different times.

In addition to the selective excitation of phonon modes, laser-stimulated surface processes of a non-selective, thermal nature can be important in such areas as annealing. The techniques for describing selective excitations can be combined with a diffusion equation to treat overall energy transfer processes.[63] Both selective and non-selective energy transfer via laser excitation of the adspecies-surface phonon modes is seen to be important. The next step in the theory of laser

induced surface dynamics would involve the inclusion of electronic degrees of freedom.

B. Charging a Semiconductor Surface

Laser excitation of the electronic degrees of freedom in the solid can stimulate rate processes by altering the charge in the vicinity of a surface. Such alteration of charge can induce desorption of an adspecies. Experiments with synchrotron radiation on metal surfaces has demonstrated this phenomena for a variety of adspecies.[64] It is reasonable to assume that reversing the charge on the surface could also enhance adsorption of the same species.

To analyze this process, a truncated one-dimensional chain has been employed.[65] Within this model and the nearly-free-electron approximation, the electronic energies are given by

$$E_k = \frac{1}{4}\{[k^2 + (k - g)^2] \pm \sqrt{[k^2 - (k - g)^2]^2 + 4E_g^2}\}, \tag{89}$$

where k is the wave vector of the electron, g is the reciprocal lattice constant, and E_g is the band gap. The plus branch represents the conduction energy band and the minus branch corresponds to the valence band. Surface states are obtained by the use of analytical continuation, i.e., the energy can also have real values for $k = g/2 + i\kappa$. Since $1/2\kappa$ is the effective charge depth of these states, they are most like surface states for large values of κ. The band structure for this system is given in Fig. 3. The band extending out of the figure represents the possible surface states.

If a laser is now shown on the linear chain, we can transfer

electrons from the valence band to the surface states. Considering the Bloch nature of our bulk states and the damped Bloch nature of our surface states, a simple analysis of the transition matrix will lead to the conclusion that the transfer is favored for bulk states at the band edge. Using this, we have calculated the absorption cross section for laser excitation of a silicon surface, and our results are depicted in Fig. 4. The glitch near the center corresponds to the maximum value of κ and is due to the branch point in the energy. Since κ is a maximum near this region, to achieve the largest surface charge density, surface states near this center should be excited. We can see from the plot that quite large cross sections ($2\text{-}3\mathring{A}^2$) can be obtained in this region at low radiation densities, (<10 W/cm^2). Thus a low-power laser is a very effective controller of surface charge.

To determine the effect of this charge on an adspecies, we have looked at the interaction of a charged adspecies with the surface.[66] The exact form of the screening function[67] at the surface can be extremely complicated; therefore, as a first approximation, we will assume that the screening is represented by an exponential damping (Thomas-Fermi screening[68]). Our results for the change in the interaction for a number of different surface state excitations are plotted in Fig. 5. It should be noted that states near the center of the band have a great deal more interaction as would be expected because of the smaller charge depth. As can be seen from the figure, both the magnitude and the range of the interaction are increased by the laser-charged surface. The attraction of the ion for the surface will thus be greatly enhanced if the ion is positive and

diminished if the ion is negative. A similar analysis could be done for polar species, with one pole being attracted and the other repelled Furthermore, a consideration of a three-dimensional semiconductor would also introduce occupied surface states. Thus raising the possibility of exciting holes into the surface, subsequently making it more positive, and producing the reverse effect of electronic excitation.

C. Electron-Phonon Coupling on Metals

In the preceding Part B, we looked at the role of increasing surface charge in semiconductors and its effect on surface dynamics. Since metals also have surface states, it would be expected that similar charge transfer induced with a laser would be possible in metallic systems.

Again using a truncated one dimensional model and the nearly-free-electron approximation,[69] the band structure for the metal will be found qualitatively similar to that of a semiconductor (see Fig. 3). However, whereas the lower band is populated to the top in a semiconductor, this band in a metal would be only partially filled. For example, for the metal sodium the top of the band is 0.7 eV above the Fermi energy. Consequently, to excite surface states in a metal, we must first overcome this energy deficit by application of a higher frequency laser than needed for semiconductors.

In a calculation of the cross section, we found that our selection rule requiring conservation of the real part of the crystal momentum still holds for metallic system. Since the top of the band is unpopulated, we would therefore expect zero transitions in the metal. However, the introduction of phonons can overcome this problem. It should be noted

that neither laser photons or lattice phonons are alone able to populate the surface states. The former will not supply sufficient crystal momentum, and the latter will not supply sufficient energy. Consequently, the absorption cross section will be second order in nature with a mixing of phonon and photon excitations. The dominant pathway would be a phonon first scattering the electron from the top of the Fermi energy to the top of the band and then a laser photon exciting this electron to the desired surface state.

The mathematics involved in the calculation of the cross section will be similar to that of the semiconductor. Because of the phonons, however, an averaging over the populated phonon states must be performed. This will give a factor depending on the phonon population multiplying our first order results:

$$\sigma^{(2)} = S\,\sigma^{(1)}. \tag{90}$$

The first-order cross section $\sigma^{(1)}$ will be comparable to that of silicon, given in Fig. 4. For sodium, the scaling factor S is about 10^{-4}. Consequently, the statements that applied for semiconductors would also be applicable to metals if the power density of our laser were 10^4 times as large. Since large cross sections were observed in the semiconductor, only a low-power laser (1-10 W/cm^2) was necessary. Therefore, only a moderate power laser (10-100 kW/cm^2) would be needed to induce surface charge transfer in a metal. Consequently, processes such as enhanced or diminished adsorption or desorption of charged or polar adspecies would also occur with similar results for metal or semiconductor surfaces.

D. Gas-Surface Charge Transfer

If a laser is used to charge a surface, we would expect the transfer of charge between the solid and an adspecies or gas molecule above the surface to be greatly enhanced.[70] Since charge transfer is the essence of chemistry, surface catalysis would be greatly effected by this phenomenon.

If we consider a positive ion impinging on a semiconductor surface, the wave function of the entire system could be approximated as a product of the wave function of the crystal and the ion. On leaving the surface, the ion could be neutralized by the transfer of charge from the surface. The final state would thus be a product of the wave functions of the neutral gas molecule and the charged substrate. If the surface of the semiconductor is first charged with a laser, the final state with the neutral gas molecule would be very favored. Fig. 6 illustrates the range over which charge transfer with the surface states can occur. The shaded curve in the figure is due to the thickness of the surface band as shown in Fig. 3. Thus, if the ion is on its initial potential curve, H_{II}, the charge neutralization process will be enhanced where this curve intersects the neutral gas-charged crystal interaction illustrated by the shaded curves. A mathematical analysis using first-order time-dependent perturbation theory will show that the neutralization rate of the ion is larger by a factor of $|2\kappa L|$ for a surface electron in state κ than for a bulk electron (L is the length of the solid).

ACKNOWLEDGMENTS

The work at the University of Rochester was supported in part by the Air Force Office of Scientific Research (AFSC), United States Air Force, under Grant AFOSR 82-0046, the Office of Naval Research, the U.S. Army Research Office and the National Science Foundation under Grant CHE-8022874. The United States Government is authorized to reproduce and distribute reprints for governmental purposes notiwthstanding any copyright notation hereon. The work at Oakland University was supported in part by the Research Corporation and an Oakland University Research Fellowship. TFG acknowledges the Camille and Henry Dreyfus Foundation for a Teacher-Scholar Award (1975-84).

REFERENCES

1. Darko, T., Baldwin, D.A., Shamir, N., Rabalais, J.W., and Hachmann, P., Reactions of homonuclear diatomic ions with metal surfaces. I. Model for X_2^+ beam-surface reactions in the low kinetic energy-near threshold region, J. Chem. Phys., 76, 6408, 1982.

2. Hagstrum, H.D., Theory of Auger ejection of electrons from metals by ions, Phys. Rev., 96, 336, 1954.

3. Merzbacher, E., Quantum Mechanics, 2nd Ed., Wiley, New York, 1970.

4. Herzberg, G., Molecular Spectra and Molecular Structure.I. Spectra of Diatomic Molecules, Van Nostrand, New York, 1950, 199,208.

5. Lundqvist, S., Electrons at metal surfaces, in Surface Science, Vol. I, International Atomic Energy Agency, Vienna, 1975, 331.

6. Kassel, L.S., Studies in homogeneous gas reactions. I., J. Phys. Chem., 32, 225, 1982.

7. Shamir, N., Baldwin, D.A., Darko, T., Rabalais, J.W., and Hochmann, P., Reaction of homonuclear diatomic ions with metal surfaces. II. Nitridation of Al, Cu, Mo, and Ni by N_2^+ beams in the low kinetic energy-near threshold region, J. Chem. Phys. 76, 6417, 1982. (see Fig. 3).

8. Tully, J.C., Dynamics of gas-surface interactions: Reaction of atomic oxygen with adsorbed carbon on platinum, J. Chem. Phys., 73, 6333, 1980.

9. Tully, J.C., Dynamics of gas-surface interactions: 3D generalized Langevin model applied to fcc and bcc surfaces, J. Chem. Phys., 73, 1975, 1980.

10. Adelman, S.A. and Doll, J.D., Generalized Langevin equation approach for atom/solid-surface scattering: General formulation for classical scattering off harmonic solids, J. Chem. Phys., 64, 2375, 1976.

11. Kubo, R., The fluctuation-dissipation theorem, Rep. Progr. Theor. Phys., 29, 255, 1966.

12. Parr, C.A. and Truhlar, D.G., Potential energy surfaces for atom transfer reactions involving hydrogen and halogens, J. Phys. Chem., 75, 1844, 1971.

13. Pollak, E., Adiabaticity and tunneling in quantal collinear reactive scattering computations, J. Chem. Phys., 75, 4435, 1981.

14. McCreery, J.H. and Wolken, G. Jr., Atomic recombination dynamics on solid surfaces: H_2 + W(001), J. Chem. Phys., 64, 2845, 1976.

15. McCreery, J.H., and Wolken, G. Jr., A model potential for chemisorption: H_2 + W(001), J. Chem. Phys., 63, 2340, 1975.

16. Erying, H., Walter, J. and Kimball, G.E., Quantum Chemistry, Wiley, New York, 1944, 232-248.

17. Anders, L.W., Hansen, R.S. and Bartell, L.S., Molecular orbital investigation of chemisorption. I. Hydrogen on tungsten(100) surface, J. Chem. Phys. 59, 5277, 1973.

18. Ziman, J.M., Principles of the Theory of Solids, Cambridge University Press, Cambridge, 1964, 27.

19. McCreery, J.H. and Wolken, G.,Jr., Atomic recombination dynamics on solid surfaces: Effect of various potentials, J. Chem. Phys., 67, 2551, 1977.

20. Diebold, A.C. and Wolken, G.,Jr., The energetics of diatom/solid dissociative adsorption, Surface Sci. 82, 245, 1979.

21. Gelb, A. and Cardillo, M.J., Classical trajectory calculations of the dissociation of hydrogen on Copper. III. The effect of surface roughness, Surface Sci., 75, 197, 1978.

22. Gregory, A.R., Gelb, A., and Silbey, R., A simple quantum chemical theory of dissociative adsorption, Surface Sci., 74, 497, 1978.

23. Gadzuk, J.W., A dissipative trajectory theory for reactive scattering at surfaces, Surface Sci., 118, 180, 1982.

24. Metiu, H. and Gadzuk, J.W., Theory of rate processes at metal surfaces. II. The role of substrate electronic excitations, J. Chem. Phys., 74, 2641, 1981.

25. Anderson, P.W., Localized magnetic states in metals, Phys. Rev., 124, 41, 1961.

26. Newns, D.M., Self-consistent model of hydrogen chemisorption, Phys. Rev., 178, 1123, 1969.

27. Schonhammer, K. and Gunnarson, O., Sticking probability on metal surfaces: Contribution from electron-hole-pair excitations, Phys. Rev. B, 22, 1629, 1980.

28. Schonhammer, K. and Gunnarson, O., Sticking and inelastic scattering at metal surfaces: The electron-hole-pair mechanism, Surface Sci., 117, 53, 1982.

29. Crjlen, Z. and Gumhatter, B., Quantum model for kinetics of helium adsorption on free-electron metals, Surface Sci., 117, 116, 1982.

30. Brako, R. and Newns, D.M., Charge exchange in atom-surface scattering: Thermal versus quantum non-adiabticity, Surface Sci., 108, 253, 1981.

31. Brako, R. and Newns, D.M., Non-adiabatic processes at metal surfaces, Vacuum 32, 39, 1982.

32. Norskov, J.K. and Lundqvist, B.I., Correlation between sticking probability and adsorbate-induced electron structure, Surface Sci., 89, 251, 1979.

33. Brenig, W., Theory of inelastic atom-surface scattering: Average energy loss and energy distribution, Z. Phys. B, 36, 81, 1979.

34. Goodman, F.O. and Wachman, H.Y., Dynamics of Gas-Surface Scattering, Academic, New York, 1976.

35. Mott, N.F. and Massey, H.S.W., Theory of Atomic Collisions, Oxford University Press, London, 1965, 792.

36. See, for example, Fano, U., Effects of configuration interaction on intensities and phase-shifts, Phys. Rev., 124, 1866, 1961.

37. Tomonaga, S., Remarks on Bloch's method of sound waves, applied to many-fermion problems, Progress. Theor. Phys., 5, 544, 1950.

38. Whaley, K.B., Light, J.C. Cowin, J.P., and Sibener, S.J., Calculation of rotationally mediated selective adsorption in molecule surface scattering: HD on Pt(111), Chem. Phys. Lett., 89, 89, 1982.

39. Yu, C.-F., Hogg, C.S., Cowin, J.P., Whaley, K.B., Light, J.C., and Sibener, S.J., to be published.

40. Glasstone, S., Laidler, K.J., and Eyring, H., The Theory of Rate Processes, McGraw Hill, New York, 1941.

41. Wigner, E., The transition state method, Trans. Faraday Soc., 34, 29, 1939.

42. Miller, W.H., Importance of nonseparability in quantum mechanical transition-state theory, Acc. Chem. Res.,9, 306, 1976.

43. Pechukas, P., Statistical approximations in collision theory, in Dynamics of Molecular Collisions, Part B., Miller, W.H., Ed., Plenum, New York, 1976, 269.

44. Kramers, H.A., Browman motion in a field of force and the diffusion model of chemical reactions, Physica, 7, 284, 1940.

45. Grimmelmann, E.K., Tully, J.C., and Helfand, E., Molecular dynamics of infrequent events: Thermal desorption of xenon from a platinum surface, J. Chem. Phys. 74, 5300, 1981.

46. Adams, J.E. and Doll, J.D., Desorption from solid surfaces via generalized Slater theory, J. Chem. Phys., 74, 1467, 1981.

47. Adams, J.E. and Doll, J.D., A Monte Carlo evaluation of thermal desorption rates, J. Chem. Phys., 74, 5332, 1981.

48. Lennard-Jones, J.E. and Strachan, C., The interaction of atoms and molecules with solid surfaces. I. The activation of adsorbed atoms to higher vibrational states, Proc. R. Soc. London, A 150, 442, 1935; Strachan, C., The interaction of atoms and molecules with solid surfaces. II. The evaporation of adsorbed atoms, Proc. R. Soc. London, A 150, 456, 1935.

49. Lennard-Jones, J.E. and Devonshire, A.F., The interaction of atoms and molecules with solid surfaces. III. The condensation and evaporation of atoms and molecules, Proc. R. Soc. London, A 156, 6, 1936; Lennard-Jones, J.E. and Devonshire, A.F., The interaction of atoms and molecules with solid surfaces. IV. The condensation and evaporation of atoms and molecules, Proc. R. Soc. London, A 156, 29, 1936.

50. Bendow, B. and Ying, S.-C., Phonon-induced desorption of adatoms from crystal surfaces. I. Formal theory, Phys. Rev. B, 7, 622, 1973; Ying, S.-C. and Bendow, B., Phonon-induced desorption of adatoms from crystal surfaces. II. Numerical computations for a model system, Phys. Rev. B, 7, 637, 1973.

51. Goodman, F.O. and Romero, I., One-phonon scattering of atoms in three dimensions by a simplified continuum model of a surface: Thermal desorption, J. Chem. Phys., 69, 1086, 1978.

52. Garrison, B.J., Diestler, D.J. and Adelman, S.A., Quantum-dynamical model for thermal desorption of gases from solid surfaces, J. Chem. Phys., 67, 4317, 1977.

53. Gortel, Z.W., Kreuzer, H.J. and Teshima, R., Desorption by phonon cascades for gas-solid systems with many physisorbed surface bound states, Phys. Rev. B, 22, 5655, 1980.

54. Gortel, Z.W., Kreuzer, H.J., Teshima, R., and Turski, L.A., Kinetic equations for desorption, Phys. Rev. B, 24, 4456, 1981; Kreuzer, H.J. and Teshima, R., Desorption times from rate equations, the master equation, and the Fokker-Planck equation, Phys. Rev. B, 24, 4470, 1981.

55. Goldys, E., Gortel, Z.W. and Kreuzer, H.J., Desorption kinetics mediated by surface photon modes, Surface Sci., 116, 33, 1982.

56. Gadzuk, J.W., Fundamental excitations in solids pertinent to desorption induced by electronic transitions, in Proceedings of DIET-I Workshop, Desorption Induced by Electronic Transitions, Tolk, N. and Traum, M. Eds., Springer-Verlag Series in Chemical Physics, 1982.

57. See, e.g., Allen, R.E., Allredge, G.P., and de Wette, F.H., Studies of vibrational surface modes. II. Monatomic fcc crystals, Phys. Rev. B, 4, 1661, 1971.

58. See, e.g., Arlinghaus, F.J., Gay, J.G., and Smith, J.R., Surface states on d-band metals, Phys. Rev. B. 23, 5152, 1981.

59. Lin, J. and George, T.F., Generalized Langevin theory of multiphoton absorption dynamics of polyatomic molecules and the nature of laser-selective effects, Phys. Lett.,80A, 296, 1980.

60. Lin, J. and George, T.F., Dynamical model of selective versus nonselective laser-stimulated surface processes, Surface Sci., 100, 381, 1980.

61. Lin, J., Beri, A.C., Hutchinson, M., Murphy, W.C., and George, T.F., Multiphoton-multiphonon theory of laser-stimulated surface processes, Phys. Lett., 79A, 233, 1980.

62. Beri, A.C. and George, T.F., Theory of laser-stimulated surface processes. I. General formulation for the multiphonon relaxation of a vibrationally excited adatom, J. Chem. Phys., 78, , 1983.

63. Lin, J. and George, T.F., Laser-generated electron emission from surfaces: Effect of the pulse shape on temperature and transient phenomena, J. Appl. Phys., 54, 382, 1983.

64. Woodruff, D.P., Traum, M.M., Farrell, H.H., Smith, N.V., Johnson, P.D., King, D.A., Benbow, R.L., and Hurych, Z., Photon- and electron-stimulated desorption from a metal surface, Phys. Rev. B.,21, 5642, 1980.

65. Murphy, W.C. and George, T.F., Laser excitation of surface electronic states for a one-dimensional semiconductor, Surface Sci., 114, 189, 1982.

66. Murphy, W.C. and George, T.F., Laser-stimulated adspecies interaction with a semiconductor surface, J. Phys. Chem., 86, 4481, 1982.

67. Newns, D.M., Dielectric response of a semi-infinite degenerate electron gas, Phys. Rev. B.,1, 3304, 1970.

68. See, e.g., Kittel, C., Quantum Theory of Solids, Wiley, New York, 1963, 105.

69. George, T.F., Lin, J., Beri, A.C., and Murphy, W.C., Theory of laser-stimulated surface processes, Prog. Surface Sci., in press.

70. Lee, H., Murphy, W.C., and George, T.F., Neutralization of ions at an electronically excited semiconductor surface, Chem. Phys. Lett., 93, 221, 1982.

Figure Captions

Fig. 1. Schematic diagram of the phonon density of states. A is the active mode, and B and C are bath modes.

Fig. 2. Average selective excitation number $\langle N_S \rangle$ as a function of time t for various values of the energy relaxation rate γ_1 for a model adspecies-surface system: (A) $10^2 s^{-1}$; (B) $10^3 s^{-1}$; (C) $2 \times 10^3 s^{-1}$; (D) $6 \times 10^3 s^{-1}$; and (E) $10^4 s^{-1}$.

Fig. 3. Dispersion relationship in complex crystal momentum space ($k + i\kappa$) for a finite linear chain. The valence, surface and conduction bands are labeled V, S and C, respectively.

Fig. 4. Absorption cross section for surface states, σ, in $\mathring{A}^2$ versus the frequency of the exciting laser radiation.

Fig. 5. Magnitude of the surface interaction potential (in millihartrees) at various distances from the surface. The solid line represents the system with excited state $\kappa \approx E_g/g$; the dashed line, $\kappa = -0.5\ E_g/g$; and the dotted line, $\kappa = -0.1\ E_g/g$, all in the lower energy branch.

Fig. 6. Schematic diagram of potential energy surfaces H_{II} and H^E_{FF} for initial and final configurations. The transfer of a surface electron to the incident ion occurs at time $t_1 \leq t \leq t_2$. For neutralization of He^* at Si(111) into the 2^3S state of He, $\Delta \approx 0.07$ eV and $E_g \approx 1.1$ eV. Shown in the inset is the square of the normalization constant, N_E^2. It assumes a maximum value when the energy E is at the center of the gap and approaches zero at both ends of the gap. This indicates that surface electrons with energy near the center of the gap are most highly localized near the surface.

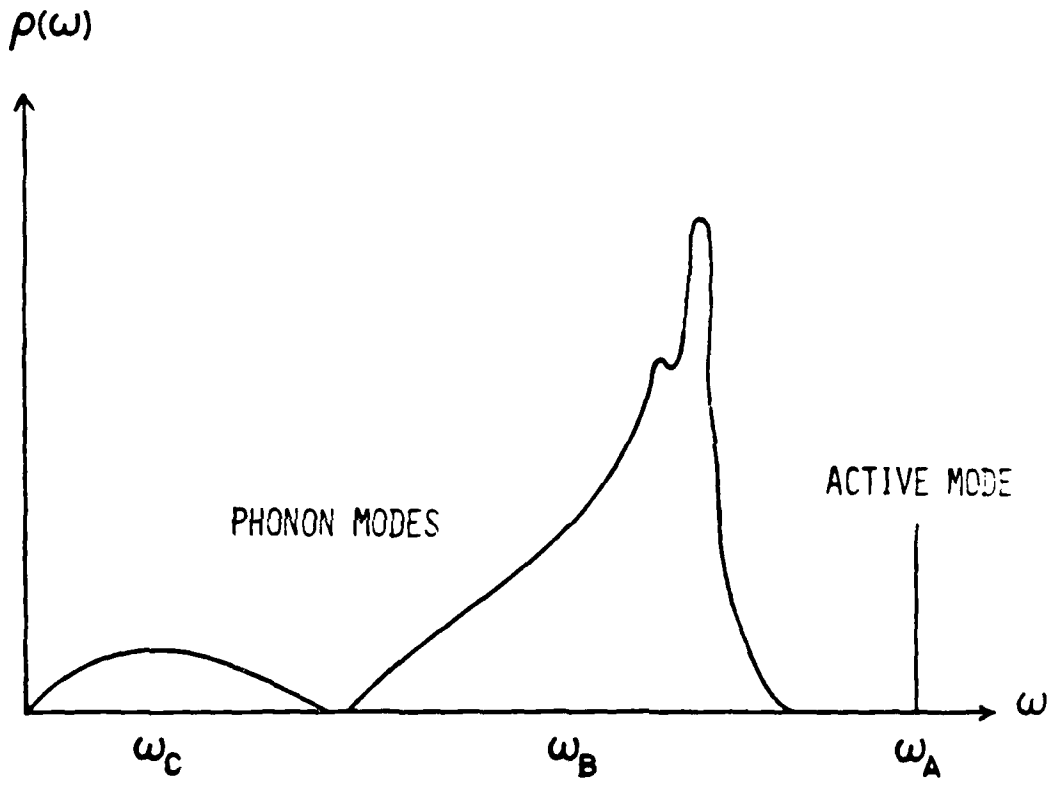

Fig. 1
Lucas et al

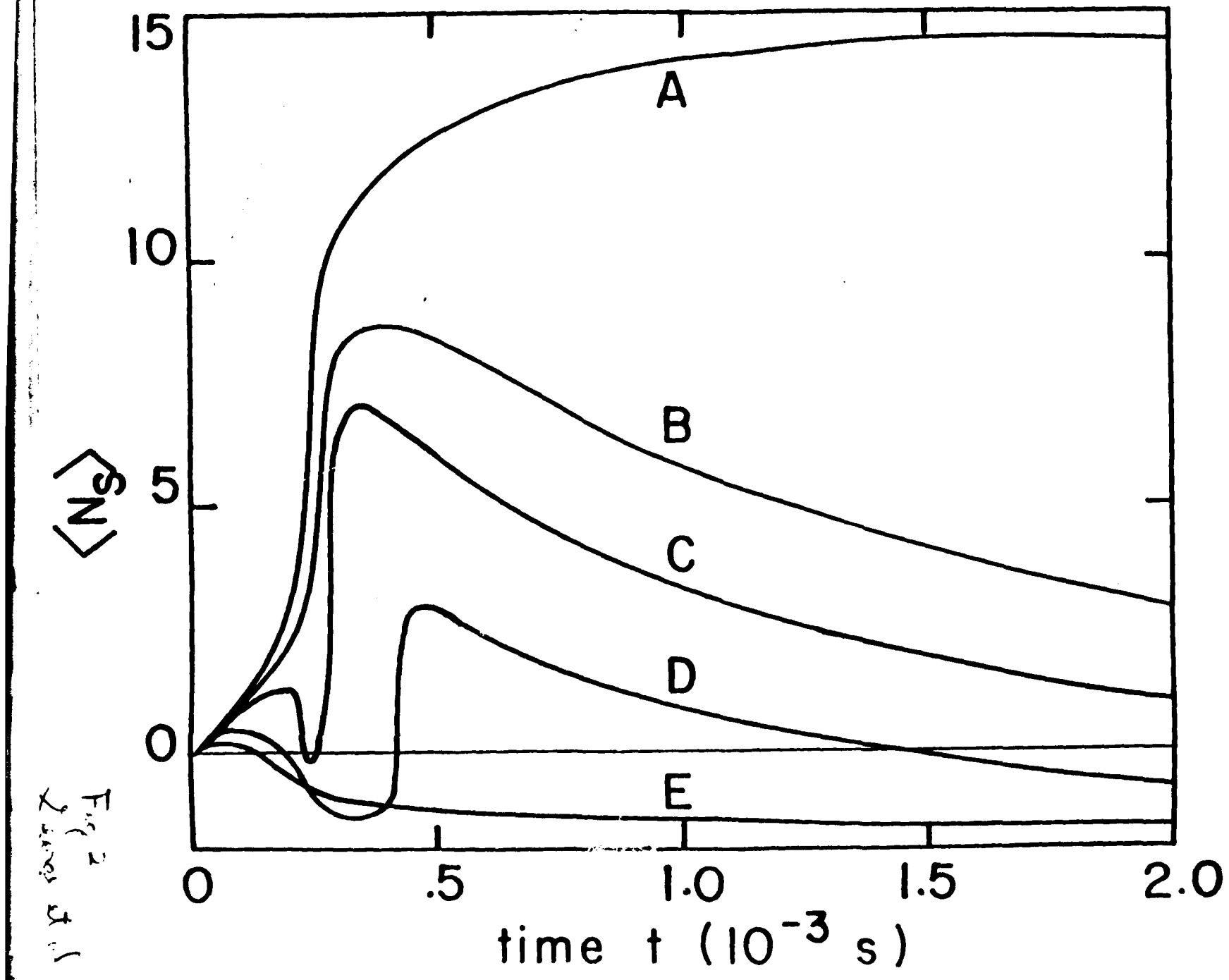
15
10
5
0
⟨Ns⟩
A
B
C
D
E
0
.5
1.0
1.5
2.0
time t (10^-3 s)

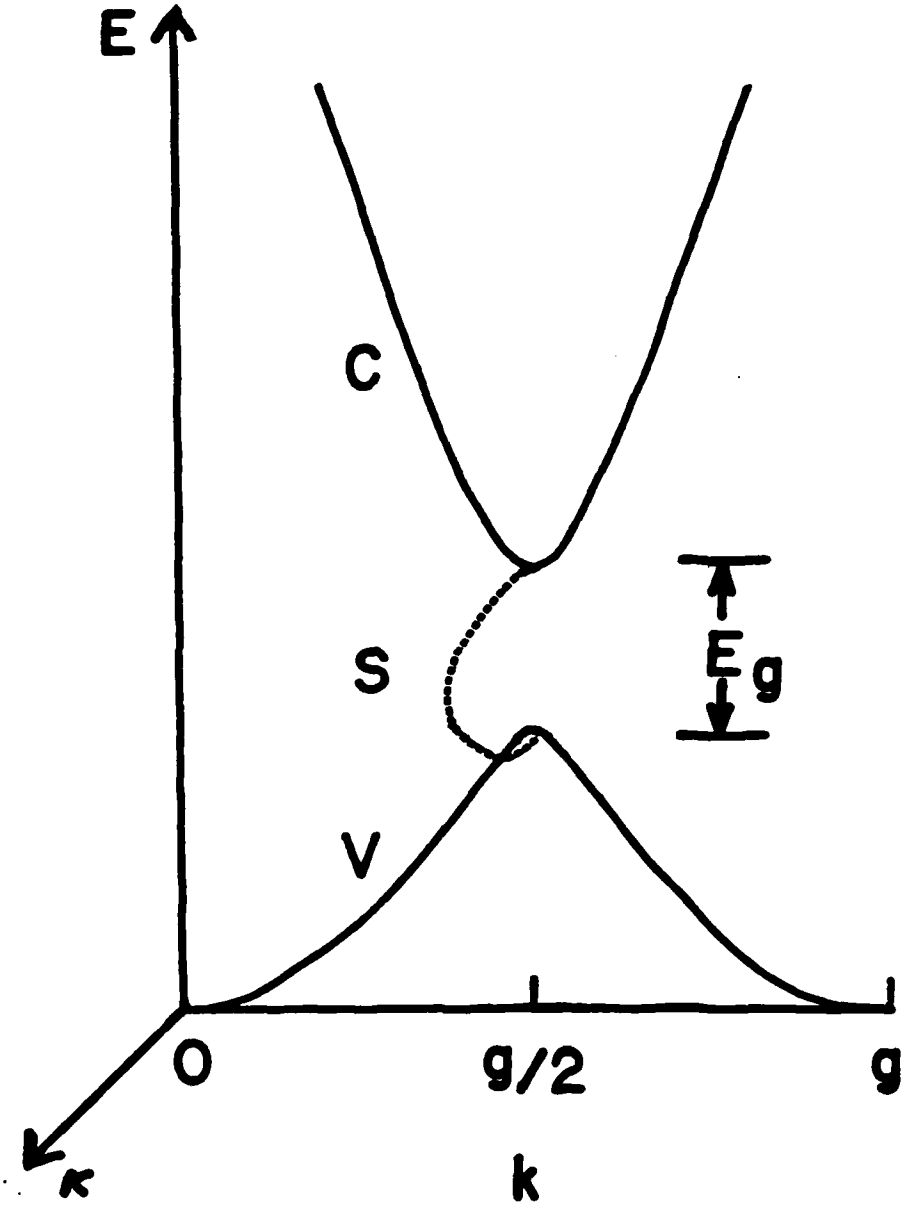

Fig. 3
Dresge et al

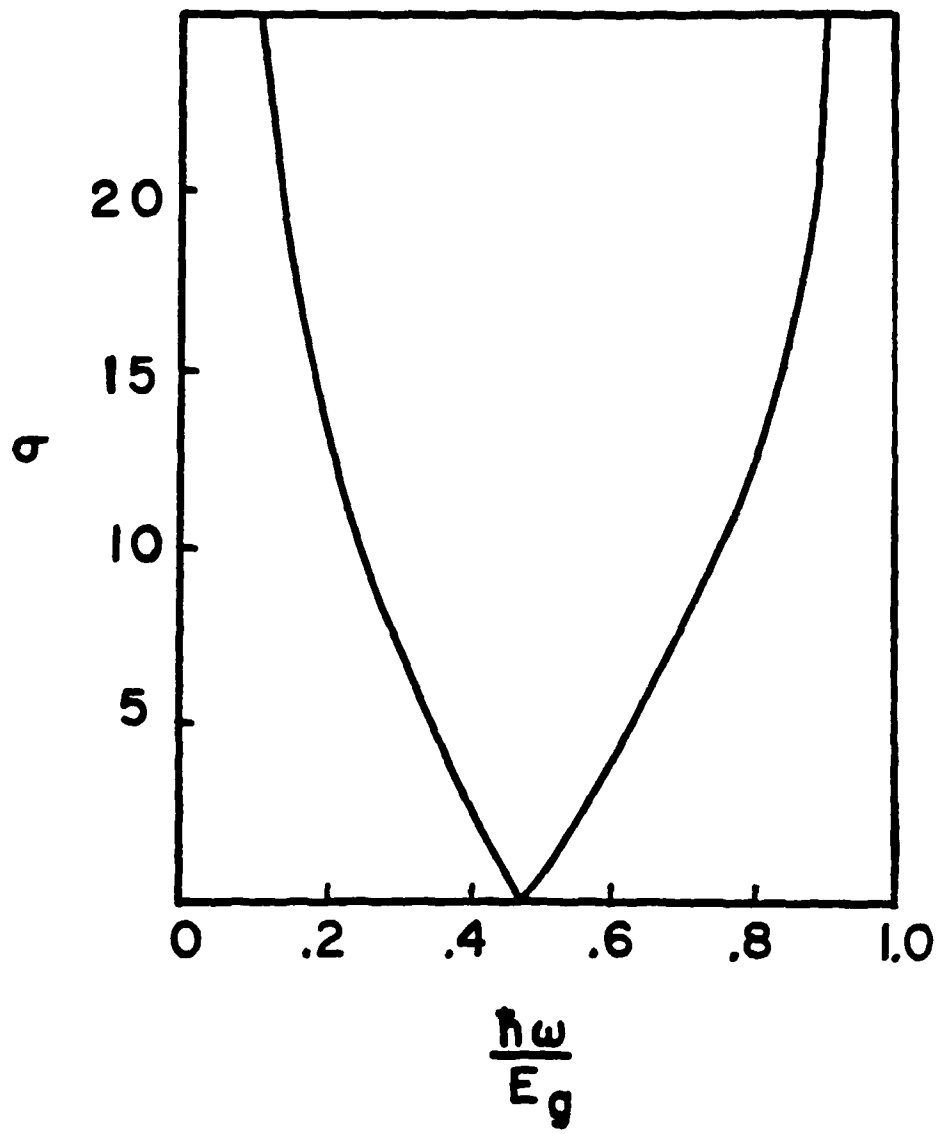

Fig. 4
Deans et al

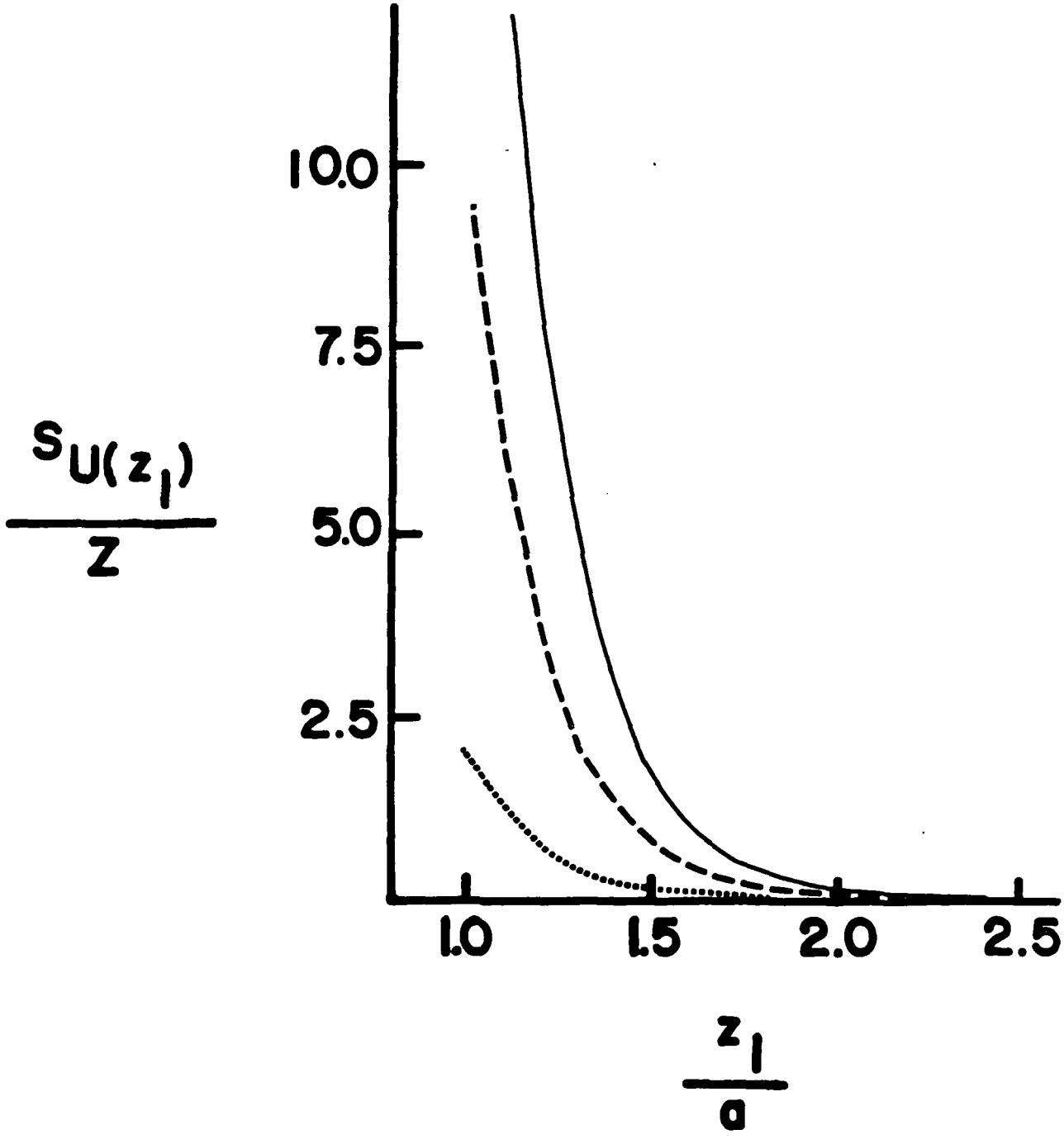

Fig. 5
George et al

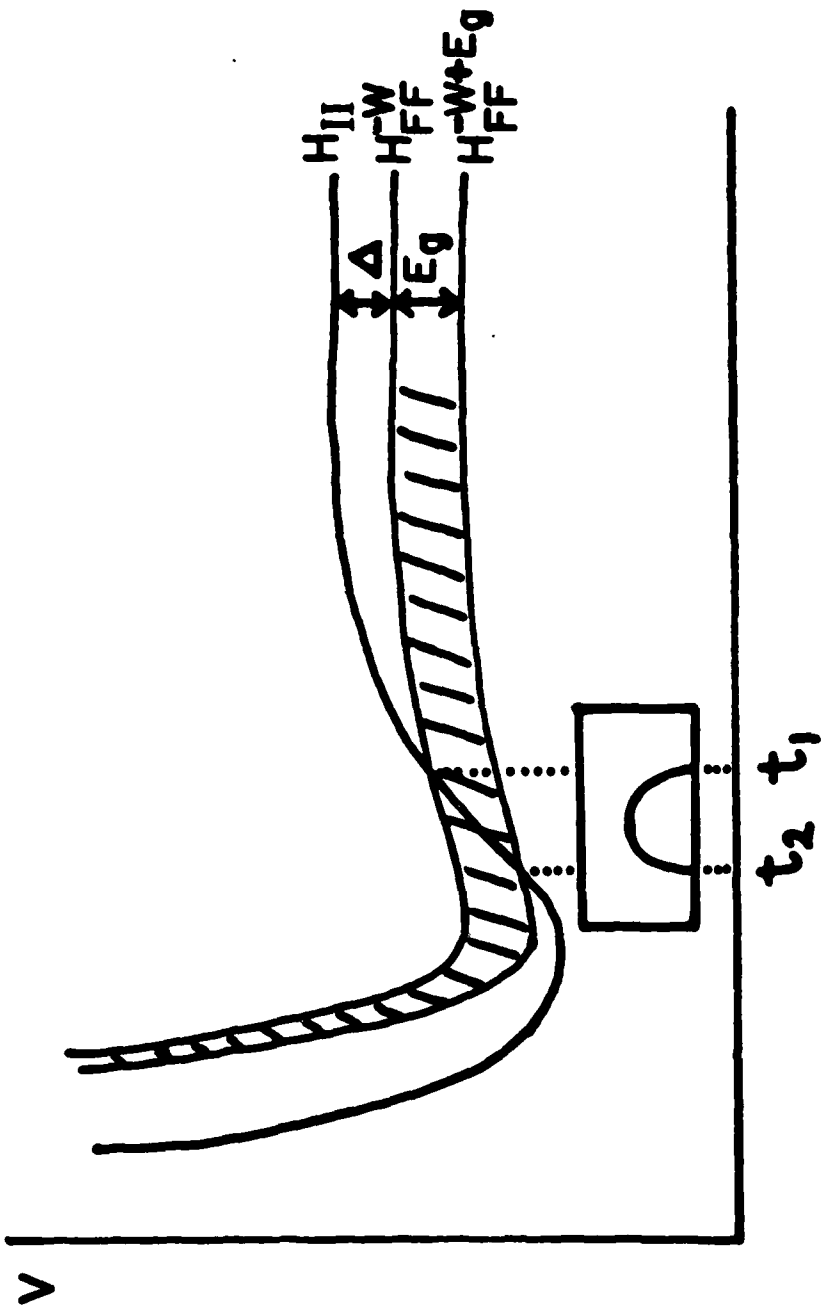

Fig. 6
Lucovsky et al

472:GAN:716-4
94/GEN

TECHNICAL REPORT DISTRIBUTION LIST, GEN

	No. Copies
Office of Naval Research Attn: Code 413 800 North Quincy Street Arlington, Virginia 22217	2
ONR Pasadena Detachment Attn: Dr. R. J. Marcus 1030 East Green Street Pasadena, California 91106	1
Commander, Naval Air Systems Command Attn: Code 310C (H. Rosenwasser) Department of the Navy Washington, D.C. 20360	1
Defense Technical Information Center Building 5, Cameron Station Alexandria, Virginia 22314	12
Dr. Fred Saalfeld Chemistry Division, Code 6100 Naval Research Laboratory Washington, D.C. 20375	1
U.S. Army Research Office Attn: CRD-AA-IP P. O. Box 12211 Research Triangle Park, N.C. 27709	1
Mr. Vincent Schaper DTNSRDC Code 2803 Annapolis, Maryland 21402	1
Naval Ocean Systems Center Attn: Dr. S. Yamamoto Marine Sciences Division San Diego, California 91232	1
Dr. David L. Nelson Chemistry Program Office of Naval Research 800 North Quincy Street Arlington, Virginia 22217	1
Naval Ocean Systems Center Attn: Mr. Joe McCartney San Diego, California 92152	1
Naval Weapons Center Attn: Dr. A. B. Amster, Chemistry Division China Lake, California 93555	1
Naval Civil Engineering Laboratory Attn: Dr. R. W. Drisko Port Hueneme, California 93401	1
Dean William Tolles Naval Postgraduate School Monterey, California 93940	1
Scientific Advisor Commandant of the Marine Corps (Code RD-1) Washington, D.C. 20380	1
Naval Ship Research and Development Center Attn: Dr. G. Bosmajian, Applied Chemistry Division Annapolis, Maryland 21401	1
Mr. John Boyle Materials Branch Naval Ship Engineering Center Philadelphia, Pennsylvania 19112	1
Mr. A. M. Anzalone Administrative Librarian PLASTEC/ARRADCOM Bldg 3401 Dover, New Jersey 07801	1

TECHNICAL REPORT DISTRIBUTION LIST, 056

	No. Copies
Dr. G. A. Somorjai Department of Chemistry University of California Berkeley, California 94720	1
Dr. J. Murday Naval Research Laboratory Surface Chemistry Division (6170) 455 Overlook Avenue, S.W. Washington, D.C. 20375	1
Dr. J. B. Hudson Materials Division Rensselaer Polytechnic Institute Troy, New York 12181	1
Dr. Theodore E. Madey Surface Chemistry Section Department of Commerce National Bureau of Standards Washington, D.C. 20234	1
Dr. J. M. White Department of Chemistry University of Texas Austin, Texas 78712	1
Dr. Keith H. Johnson Department of Metallurgy and Materials Science Massachusetts Institute of Technology Cambridge, Massachusetts 02139	1
Dr. J. E. Demuth IBM Corporation Thomas J. Watson Research Center P. O. Box 218 Yorktown Heights, New York 10598	1
Dr. C. P. Flynn Department of Physics University of Illinois Urbana, Illinois 61801	1
Dr. W. Kohn Department of Physics University of California (San Diego) La Jolla, California 92037	1
Dr. R. L. Park Director, Center of Materials Research University of Maryland College Park, Maryland 20742	1
Dr. W. T. Peria Electrical Engineering Department University of Minnesota Minneapolis, Minnesota 55455	1
Dr. Chia-wei Woo Department of Physics Northwestern University Evanston, Illinois 60201	1
Dr. Robert M. Hexter Department of Chemistry University of Minnesota Minneapolis, Minnesota 55455	1
Dr. R. P. Van Duyne Chemistry Department Northwestern University Evanston, Illinois 60201	1
Dr. S. Sibener Department of Chemistry James Franck Institute 5640 Ellis Avenue Chicago, Illinois 60637	1
Dr. M. G. Lagally Department of Metallurgical and Mining Engineering University of Wisconsin Madison, Wisconsin 53706	1

TECHNICAL REPORT DISTRIBUTION LIST, 056

	No. Copies
Dr. Robert Gomer Department of Chemistry James Franck Institute 5640 Ellis Avenue Chicago, Illinois 60637	1
Dr. R. G. Wallis Department of Physics University of California, Irvine Irvine, California 92664	1
Dr. D. Ramaker Chemistry Department George Washington University Washington, D.C. 20052	1
Dr. P. Hansma Physics Department University of California, Santa Barbara Santa Barbara, California 93106	1
Dr. J. C. Hemminger Chemistry Department University of California, Irvine Irvine, California 92717	1
Dr. Martin Fleischmann Department of Chemistry Southampton University Southampton SO9 5NH Hampshire, England	1
Dr. G. Rubloff IBM Thomas J. Watson Research Center P. O. Box 218 Yorktown Heights, New York 10598	1
Dr. J. A. Gardner Department of Physics Oregon State University Corvallis, Oregon 97331	1
Dr. G. D. Stein Mechanical Engineering Department Northwestern University Evanston, Illinois 60201	1
Dr. K. G. Spears Chemistry Department Northwestern University Evanston, Illinois 60201	1
Dr. R. W. Plummer University of Pennsylvania Department of Physics Philadelphia, Pennsylvania 19104	1
Dr. E. Yeager Department of Chemistry Case Western Reserve University Cleveland, Ohio 41106	1
Professor D. Hercules University of Pittsburgh Chemistry Department Pittsburgh, Pennsylvania 15260	1
Professor N. Winograd The Pennsylvania State University Department of Chemistry University Park, Pennsylvania 16802	1
Professor T. F. George The University of Rochester Chemistry Department Rochester, New York 14627	1
Professor Dudley R. Herschbach Harvard College Office for Research Contracts 1350 Massachusetts Avenue Cambridge, Massachusetts 02138	1
Professor Horia Metiu University of California, Santa Barbara Chemistry Department Santa Barbara, California 93106	1
Professor A. Steckl Rensselaer Polytechnic Institute Department of Electrical and Systems Engineering Integrated Circuits Laboratories Troy, New York 12181	1

472:GAN:716-4
94/056

TECHNICAL REPORT DISTRIBUTION LIST, 056

	No. Copies	No. Copies
Dr. John T. Yates Department of Chemistry University of Pittsburgh Pittsburgh, Pennsylvania 15260	1	
Professor G. H. Morrison Department of Chemistry Cornell University Ithaca, New York 14853	1	
Captain Lee Myers AFOSR/NC Bolling AFB Washington, D.C. 20332	1	
Dr. David Squire Army Research Office P. O. Box 12211 Research Triangle Park, NC 27709	1	
Professor Ronald Hoffman Department of Chemistry Cornell University Ithaca, New York 14853	1	